



THE UNIVERSITY OF
WAIKATO
Te Whare Wānanga o Waikato

Research Commons

<http://waikato.researchgateway.ac.nz/>

Research Commons at the University of Waikato

Copyright Statement:

The digital copy of this thesis is protected by the Copyright Act 1994 (New Zealand).

The thesis may be consulted by you, provided you comply with the provisions of the Act and the following conditions of use:

- Any use you make of these documents or images must be for research or private study purposes only, and you may not make them available to any other person.
- Authors control the copyright of their thesis. You will recognise the author's right to be identified as the author of the thesis, and due acknowledgement will be made to the author where appropriate.
- You will obtain the author's permission before publishing any material from the thesis.

**The Effect of Heat Treatment on the Structure and Properties of
Hemp/PLA Composites**



THE UNIVERSITY OF
WAIKATO
Te Whare Wānanga o Waikato

A thesis
submitted in fulfilment
of the requirements for the degree
of
Master of Engineering
at
The University of Waikato

by
Jeevan Jayaraman

The University of Waikato,
Hamilton, New Zealand

April 2010

Addendum

Title of Thesis: The Effect of Heat Treatment on the Structure and Properties of Hemp/PLA Composites

Name: Jeevan Jayaraman

Institution: The University of Waikato, Hamilton, New Zealand

Course: Master of Engineering

Date of Submission: April 2010

EXPLANATORY NOTE: The pages of the thesis listed below have been superseded by the pages attached on the back of the relevant preceding pages and are numbered as stated:-

Delete Page 40: replace with Page 40a

Delete Page 47: replace with Page 47a

Delete Page 52: replaced with Page 52a

Delete Pages 60 and 61: replace with Pages 60a and 61a

Delete Page 77: replace with Page 77a

Abstract

This project focuses on bio-derived composites made from poly(lactic acid) (PLA) and hemp as well as the influence of PLA crystallinity on material properties.

It is known that crystallinity can occur as spherulites within a polymer matrix bulk and as transcristallinity on fibre surfaces in thermoplastic matrix composites. In addition, thermal history is known to influence the degree of crystallinity of polymer materials. The aim of this project was to study the effect of heat treatment or “annealing” on crystallinity and the influence of this on properties of hemp/PLA composites.

Composites were observed to become more opaque during heat treatment and increased crystallinity after heat treatment was seen using optical microscopy. XRD and DSC results showed that crystallinity was much higher for composites than PLA, supporting the fibre acting as a nucleating agent. There was no apparent change to tensile strength with increased heat treatment for PLA, however, for composite samples, increased heat treatment led to a small reduction in average tensile strength. Although there was no discernable trend for change of fracture toughness with increased crystallinity for PLA, it decreased for composite materials. It appears that the increased crystallinity present in the composite in combination with increased stress concentration due to the presence of fibres is reducing composite toughness as well as leading to premature failure in tensile tests due to PLA brittleness explaining lower strengths for composites. DMTA suggests that increase in crystallinity contributes to thermal stability of the composite.

Acknowledgments

There are many things I have gained throughout the course of this thesis; many things of which I must be thankful for learning, and many people I have much appreciation for.

First off, I offer my deepest gratitude to my parents, whom have always supported me throughout this journey of life. I offer my humblest appreciation and gratitude to my supervisor, Associate Professor Kim Pickering for giving me the opportunity and support in doing this thesis topic, and for giving me valuable insight and guidance.

I would like to thank the whole research team of the Materials Engineering department too, especially Jim Bier and Amro Gazawi for their help and support as well as their comradeship. Also, I thank Paul Ewart, Yuanji Zhang, Indar Singh, and Helen Turner for their technical support and assistance.

Table of Contents

Abstract.....	i
Acknowledgements.....	ii
Table of Contents.....	iii
List of Figures.....	vi
List of Tables.....	ix
List of Abbreviations	x
Chapter 1: Introduction	
1.1 Overview of Composite Materials and Natural Fibres.....	1
1.2 Thermoplastics of Natural Origin and their Composites.....	2
1.3 Crystallinity and Heat Treatment.....	3
1.4 State of Research and Research Objectives	3
Chapter 2: Literature Review	
2.1 Natural Fibre, Hemp Fibre and its constituents.....	5
2.1.1 Natural Fibre Composites.....	5
2.1.2 Hemp Fibre and Morphology.....	9
2.1.3 Hemp Fibre: its Constituents.....	11
2.1.3.1 Cellulose.....	11
2.1.3.2 Hemicellulose.....	12
2.1.3.3 Lignin.....	13
2.1.3.4 Pectin.....	13
2.1.4 Degradability of Hemp fibre.....	14
2.2 Bio-derived Thermoplastics.....	14
2.2.1 Poly (Lactic Acid) and its Sources.....	16
2.2.2 The Biodegradability of PLA.....	19
2.3 Issues with the use of Natural Fibres in Bio-derived Matrix Composites	19
2.3.1 Cellulose-based Natural Fibres and its Issues.....	19
2.3.2 Bio-derived Matrices and their Issues.....	20
2.3.3 Hemp/PLA Fibre Composite and their Issues.....	20
2.4 Process and Manufacture of Composites.....	22

2.4.1 Basic processes of preparing composites.....	21
2.4.1.1 Alkali treatments.....	22
2.4.1.2 Acetylation.....	22
2.4.1.3 Silane treatments.....	22
2.4.1.4 Matrix treatments.....	23
2.4.2 Basic Manufacture of Composites.....	23
2.4.2.1 Melt mixing.....	24
2.4.2.2 Extrusion.....	24
2.4.2.2 Injection Moulding.....	26
2.4.2.3 Compression Moulding.....	28
2.4.3 Process and Manufacture of Hemp/PLA Fibre.....	29
2.5 Crystallinity of Polymers and Composite materials.	30
2.5.1 Crystallinity of Polymers.....	30
2.5.2 Crystallinity in PLA and its Composites.....	31
2.6 Physical and Mechanical Characterisation Methods.....	31
Chapter 3: Materials and Methods	
3.1 Experimental Overview.....	33
3.2 Materials used.....	33
3.2.1 Hemp Fibre and its Treatment.....	34
3.2.2 Poly(lactic acid) (PLA)	34
3.3 Fabrication and Post Treatment of Composites.....	34
3.4 Treatment of Fabricated Composites.....	36
3.5 Analysis of Composites.....	37
3.5.1 Scanning Electron Microscope (SEM)	37
3.5.2 Differential Scanning Calorimetry (DSC)	37
3.5.3 X-Ray Diffraction Analysis (XRD)	38
3.5.4 Polarised Optical Microscope (POM)	39
3.5.5 Fracture Toughness (K_{1C}) and Tensile Testing.....	39
3.5.6 Dynamic Mechanical Thermal Analysis (DMTA)	41

Chapter 4: Results and Discussion	
4.1 Introduction	43
4.2 Experimental Results and Discussion.....	44
4.2.1 Scanning Electron Microscope (SEM) Analysis.....	44
4.2.2 Differential Scanning Calorimetry (DSC)	48
4.2.3 X-Ray Diffraction (XRD) Analysis	52
4.2.4 Polarised Optical Microscope (POM) Analysis.....	54
4.2.5 Tensile Strength and Fracture Toughness (K_{1C})	57
4.2.6 Dynamic Mechanical Thermal Analysis (DMTA)	61
 Chapter 5: Conclusions and Recommendations for Future Work	
5.1 Conclusions.....	65
5.2 Recommendations for Future Work	66
References.....	67
Appendices.....	77

List of Figures

Figure 2.1 A comparison of the varieties of hemp plant. Left : industrial hemp, Right: medical/hallucigenic hemp [26]	10
Figure 2.2 Schematic of hemp plant stalk [13].....	10
Figure 2.3 Chemical structure of cellulose [115].....	11
Figure 2.4 Schematic diagram of cellulose fibres [115].....	12
Figure 2.5 Hemicellulose molecular structures [116].....	12
Figure 2.6 Lignin molecular structure [116].....	13
Figure 2.7 Pectin molecular and unitary arrangement [117].....	14
Figure 2.8 PLA monomer and polymerisation [118].....	16
Figure 2.9 Stereo-isomeric structures of lactide.....	17
Figure 2.10 Poly (lactic Acid) flow chart; from cradle to grave [44].....	18
Figure 2.11 The Extruder [62].....	24
Figure 2.12 Injection Moulding(a) loading melt chamber (b) inject material into mould [62].....	26
Figure 2.13 Compression mould schematic diagram [62].....	28
Figure 2.14 Schematic diagram of polymer chain alignments [38].....	30
Figure 3.1 Fibre/PLA mix prior to compounding in extruder	34
Figure 3.2 Fibre/PLA mix being fed down the extruder's hopper.....	34
Figure 3.3: Extruder where composite is compounded	35
Figure 3.4 Compounded hemp/PLA extrude prior to being granulated.....	35
Figure 3.5 Boy15-S Injection moulding machine.....	35
Figure 3.6 Some of the fracture toughness testing samples.....	35
Figure 3.7 Left: Glass slip-slide prior to being pressed Right: After pressing..	35
Figure 3.8 Annealed samples of PLA.....	36
Figure 3.9 Annealed samples of 15% wt hemp/PLA	36
Figure 3.10 Annealed samples of 30% wt hemp/PLA	36
Figure 3.11 The SEM.....	37
Figure 3.12 Aluminium stubs with mounted platinum/ palladium sputtered test pieces.....	37
Figure 3.13 Differential scanning calorimetry machine.....	38
Figure 3.14 Polarised Optical Microscope setup.....	39
Figure 3.15 Single fibre/PLA glass slide samples.....	39

Figure 3.16 Fracture toughness sample with notch.....	40
Figure 3.17 Diagram representing a 3 point Single End Notch Bending fracture toughness configuration.	40
Figure 3.18 Tensile testing samples.....	41
Figure 3.19 Instron universal testing machine for tensile testing	41
Figure 3.20 Dynamic mechanical analyser during a test run.....	42
Figure 3.21 Dynamic mechanical analyser test apparatus set-up, single end cantilever.	42
Figure 4.1 Annealed samples of PLA.....	43
Figure 4.2 Annealed samples 15% wt hemp/PLA	44
Figure 4.3 Annealed samples 30% wt hemp/PLA	44
Figure 4.4 SEM of fracture surface of PLA control sample at 10mm/min.....	44
Figure 4.5 SEM of fracture surface of PLA 100°C 24hrs sample at 10mm/min.....	45
Figure 4.6 SEM of fracture surface of 15 wt% hemp/PLA control sample at 10mm/min.....	45
Figure 4.7 SEM of fracture surface of 15 wt% hemp/PLA 100°C 24hrs sample at 10mm/min.....	46
Figure 4.8 SEM of fracture surface of 30 wt% hemp/PLA control sample at 10mm/min.....	46
Figure 4.9 SEM of fracture surface of 30 wt% hemp/PLA 100°C 24hrs sample at 10mm/min.....	47
Figure 4.10 PLA DSC thermograph.....	48
Figure 4.11 15 wt% hemp/PLA DSC thermograph.....	49
Figure 4.12 30 wt% hemp/PLA variants thermograph.....	49
Figure 4.13 Percentage crystallinity graph for control and treated samples of PLA and composites.....	52
Figure 4.14 XRD diffractrogram of hemp/PLA composites.....	53
Figure 4.15 fibres embedded in PLA between two glass slips(200x magnification): a): Untreated fibre b): Treated fibre in PLA...	55
Figure 4.16 Fracture toughness samples showing crack profiles for a) PLA control b) PLA annealed 100°C 24hrs.....	55

Figure 4.17 Fracture toughness samples showing crack profiles for, a)- 15 wt% hemp/ PLA b)- 15 wt% hemp/PLA 100°C 24 hours.....	56
Figure 4.18 Fracture toughness samples showing crack profiles for a)- 30 wt% hemp/PLA, b)- 30 wt% hemp/PLA 100°C 24 hours.....	57
Figure 4.19: a) Tensile strength for hemp/PLA composites at 10mm/min b)Tensile strength vs. crystallinity for hemp/PLA composites..	58
Figure 4.20: a)Failure strain (%) for hemp/PLA composites at 10mm/min, b) Failure strain (%) vs. crystallinity for hemp/PLA composites...	58
Figure 4.21: a) Young's modulus values for hemp/PLA composites at 10mm/min, b) Young's modulus vs. crystallinity (%) for hemp/PLA composites.....	59
Figure 4.22: a) Fracture toughness for hemp PLA composites at 10mm/min, b) Fracture toughness vs. crystallinity for hemp/PLA composites.....	60
Figure 4.23 E', E'' and tan δ for PLA control at 1Hz and 10Hz.....	62
Figure 4.24 E', E'' and tan δ for PLA 100°C 24Hrs at 1Hz and 10Hz.....	62
Figure 4.25 E', E'' and tan δ for 15 wt % hemp/PLA control at 1Hz and 10Hz	63
Figure 4.26 E', E'' and tan δ for 15 wt % hemp/PLA 100°C 24Hrs at 1Hz and 10Hz.....	64
Figure 4.27 E', E'' and tan δ for 30 wt % hemp/PLA control at 1Hz and 10Hz	64
Figure 4.28 E', E'' and tan δ for 30 wt % hemp/PLA 100°C 24Hrs at 1Hz and 10Hz.....	64
Appendix 5 Data from Dynamic Mechanical Thermal Analysis Static and Dynamic Force, with Static Displacement graphs.....	81 -
	82

List of Abbreviations and Symbols

PLA	Poly(lactic acid)
DSC	Differential Scanning Calorimetry
XRD	X-ray Diffraction
SEM	Scanning Electron Microscopy
ASTM	American Society for Testing and Materials
POM	Polarised Optical Microscope
DMTA	Dynamic Mechanical Analysis
GMT	Glass-fibre Mat Thermoplastic
HMT	Hemp-fibre Mat Thermoplastic
SENB	Single-edge notched bending
X_{DSC}	Crystallinity
GPa	Gigapascal
K_Q	Stress-intensity factor
K_{IC}	Critical stress-intensity factor
E	Young's modulus
E'	Storage modulus
E''	Loss modulus
$\tan \delta$	Mechanical damping factor
σ	Stress
ε	Strain
T_G	Glass transition temperature
T_{CC}	Cold crystallinity temperature
T_m	Melting temperature
ΔH_{CC}	Cold crystallisation enthalpy
ΔH_M	Enthalpy of melting

Chapter 1: Introduction

1.1 Overview of Composite Materials and Natural Fibres

A composite material contains two or more distinct materials as a united construction. The best structural performance is obtained from those composites that contain fibres. When high temperature performance is not required, a polymer matrix is generally utilised as it is the easiest to process and is lightweight. The polymer, therefore, does not detract dramatically from the specific strength and stiffness of the fibres [1].

Composite materials have been around for many millennia. The first recorded usage of fibre reinforced material has been found to be depicted on the walls of Egyptian tombs, demonstrating the use of straw reinforced clay bricks. Here the addition of straw made the bricks lighter and offered insulation. The Sub-Continental Indians and various cultures around the world have traditionally used mud and straw faced floors and bricks/walls made from clay and straw. The Mongolians have used composites made from wood, bullock tendon and corn fibre with pine resin as an adhesive to craft high precision and powerful bows [2].

Recently, there has been a return to using renewable natural fibres as filler/reinforcement material in various composites. One of the main drivers for this is the increase in environmental protection consciousness. The production of traditional reinforcing fibres such as glass fibre and petroleum-derived fibres (e.g. nylon) uses a lot of energy and adversely affects the environment [4]. The disposal of these traditional reinforcement fibres also causes many problems as they are not biodegradable. Therefore, natural fibres are seen as an important replacement material.

Currently, natural fibres are used primarily in vehicle panelling, sound insulation and seating, replacing materials such as wood or polymer [3]. This allows for significant reduction in production cost and in service, lower vehicle mass and thus overall lower energy consumption. Also, natural fibres are renewable and relatively easily disposed of or potentially recycled at the end of their lifecycle [5].

1.2 Thermoplastics of Natural Origin and their Composites

Thermoplastics of natural origin have great potential in sustainable technological development. They are desirable as they can be used in current petroleum-based thermoplastic processes and machinery with little or no change in procedure [6]. There are a number of types of bio-plastics that meet this criterion with current commercial focus on plastics that are of plant origin, such as poly(lactic acid) (PLA), cornstarch plastics and corn gluten meal. The biodegradable aspects of such plastics are crucial to their success in replacing traditional plastics. Currently, PLA derived from a corn feedstock is one of the most widely used biodegradable bio-derived polymers in industry to replace standard petroleum thermoplastics.

Composites made from biodegradable bio-derived thermoplastics and natural fibres have the potential to be composted or degraded without need for separation/refining. They have comparable mechanical properties to traditional composites such as glass fibre reinforced polymer. However, there are some drawbacks associated with natural fibre reinforced bio-derived polymer composites, mainly being their moisture resistance and poor compatibility of their constituent materials [7]. It would also be anticipated that due to the brittleness of PLA, composites using it as a matrix may be brittle.

1.3 Crystallinity and Heat Treatment

Crystallinity can occur in many thermoplastic polymers; it is a phenomenon where segments within the polymer chain either align themselves in an orderly, structured fashion or align themselves with portions of adjacent polymer chains in a similar fashion. The degree of crystallinity influences material properties such as hardness, tensile, strength, stiffness, toughness, impact resistance, melting point and their ability to act as a chemical barrier [8].

Crystallinity does not exist when the polymer is above its melting point. As the polymer temperature drops below the melting point, it begins to crystallise. The faster the cooling rate, the lower the overall degree of crystallinity that occurs and conversely, the slower a polymer cools, the higher the degree of crystallinity within the polymer [9]. It follows that by controlling cooling duration and temperature, control of crystallinity could be achieved. In addition, heat treatment post manufacture affects materials in various ways and could be used to control crystallinity. Other than using heat treatment, the addition of nucleating agents such as talc and micro-sized particles can be used to induce crystallinity [10]. Further, crystallinity has been shown to be induced due to the presence of natural cellulose-based fibres [86].

1.4 State of Research and Research Objectives

To enable optimisation of material properties of hemp/PLA composites, it is important to understand the relationship between crystallinity and material properties. Therefore, the purpose of this research is to evaluate the viability of controlling crystallinity in hemp/PLA composites using heat treatment and to determine the influence of crystallinity on material properties of hemp/PLA

composites. The outlines of the research plan to achieve the above goals are as follows:

- Production and heat treatment of hemp/PLA composites for tensile and fracture toughness testing
- To study the physical and mechanical characteristics of the heat treated Hemp/PLA samples using Differential Scanning Calorimetry (DSC), Scanning Electron Microscopy (SEM), Dynamic Mechanical Thermal Analysis (DMTA) and X-ray diffraction (XRD) analysis.
- To study the effects of crystallinity on material properties of Hemp/PLA composites

Chapter One presents a general introduction to the research objective and rationale. Chapter Two presents a relevant literature review of natural composites and hemp, poly (lactic acid), crystallinity in polymers and issues regarding use of composite materials. Chapter Three covers details of material, fibre treatment methods, composite processing and mechanical and physical characterisation of composites. Chapter Four has the results and discussion for the work carried out. Chapter Five is the conclusion of the thesis and puts forth suggestions and recommendations for future work.

Chapter 2: Literature Review

2.1 Natural Fibre, Hemp Fibre and its Constituents

2.1.1 Natural Fibre Composites

Natural fibres have become more important to the composites industry over the past few decades due to their advantages over more traditional engineering fibres such as glass fibres or fibres made from petroleum feedstock. These include weight saving, lower raw material prices, ease of recycling, availability of fibres, specific properties that are similar to non-renewable fibres and biodegradability [11].

Natural fibres can be derived from either animal or plant sources. With the exception of wool and silk, most natural textile fibres are plant derived. Generally, plant fibres are cellulose-based, whereas fibres of animal origin consist of proteins. Natural cellulose-based fibres tend to be stronger and stiffer than animal fibres, and are therefore more suitable for use in composite materials [12]. Depending on the origin of the fibre, cellulose-based fibres can be classified into the following categories:

- Grasses and reeds, for example, bamboo, cereal, sugar cane, papyrus.
- Leaf fibres, for example from sisal and abaca.
- Bast Fibres, such as jute, flax, hemp and kenaf.
- Seed and fruit hairs, two being cotton and coconut.
- Wood fibres, including pine, maple and spruce.

Some materials that are used for reinforcing a thermoplastic matrix are presented in Table 2.1 along with some referenced data [5, 13].

Table 2.1 – Mechanical Properties of Fibres [5, 13]

Fibre type	Density (kg/m ³)	Tensile strength (MPa)	Specific Strength (kN.m/kg)	Young's Modulus (GPa)	Specific Stiffness (MN.m/kg)
Jute	1.3	393	302	55	21
Coir	1.25	220	176	6	5
Sisal	1.3	510	392	28	22
Flax	1.5	344	229	27	18
Hemp	1.07	389 -750	364- 701	35-70	33-65
Cotton	1.51	400	265	12	8
Glass Fibre-E	2.5	3400	1360	72	28

It is observed that the tensile strength of glass fibre is significantly higher than that for natural fibres. Conversely, when the specific stiffness (Young's modulus/density) is considered, it is found that most natural fibres show comparable or superior values to that of glass fibre. These values show that natural fibres can replace glass fibres in order to reduce product mass, while retaining similar or superior specific stiffness along with an acceptable specific strength.

In addition to favourable material properties, the overall energy cycle for fibre production is balanced, taking into consideration that natural fibres have high calorific values. This enables energy recovery in the form of incineration at the end of the natural fibre product's service life. In a study carried out by Sain et.al [4], hemp reinforced polypropylene composites consisting of 65wt% fibre were calculated to consume 30,800 MJ of energy per ton of composite, whereas glass fibre reinforced polypropylene (PP) composites consumed 81,890MJ/ton of

energy, nearly 3 times more than that of natural fibres, as illustrated in the following Table 2.2 .

Table 2.2: Overall energy schedule for hemp fibre mat thermoplastic (HMT) composites and glass fibre mat thermoplastic (GMT) composites [4]

Quantity (per metric ton)	HMT (65wt% fibre)	Energy (MJ)	GMT (30 wt% fibre)	Energy (MJ)
(a) Materials				
	Hemp cultivation	1 340	Glass fibre production	14 500
	PP production	35 350	PP production	70 700
	Total	36 690	Total	85 200
(b) Production				
	Composite	11 200	Composite	11 200
(c) Incineration				
	PP incineration		PP incineration	
	Energy required	117	Energy required	234
	Energy released	-7 630	Energy released	-15 260
	Hemp fibre incineration		Glass fibre incineration	
	Energy required	1 108	Energy required	516
	Energy released	-10 650		
	Net	-17 055	Net	-14 510
(d) Balance				
	Gross energy required	49 115	Gross energy required	97 150
	Energy released	-18 222	Energy released	-15 260
	Net energy required	30 800	Net energy required	81 890

CO₂ is purported to be a major cause of what is known as the greenhouse effect observed in the world, causing drastic climate change [15]. Most plant derived fibres can be considered to be neutral in CO₂ their lifetime, as they utilise CO₂ during the growing stage. This means that natural fibres can be burned at the

end of their lifespan, while keeping the amount of CO₂ in the atmosphere the same. Alternatively, burning petroleum-derived fibres release previously “locked-in” CO₂ into the atmosphere, causing a net increase of CO₂, which would be best avoided.

When a composite component fractures, particles of fibre are released into its surroundings; in the case of glass fibre reinforced composites, splinters of glass fibre are released and become a safety hazard, both respiratory and externally [16]. However, natural fibre reinforced composites rarely have adverse effects to the respiratory system or externally, and do not shatter or splinter upon fracturing [14] [17]. This makes the natural fibre reinforced composite a safe material to be used in crash absorbing applications or any application that has a risk of failure, and requires a sacrificial component.

Cost and ease of availability are crucial to selecting reinforcement fibres. Most natural fibres are easily produced around the world at low cost, especially in developing countries [18]. They require very little capital investment, little or no mechanisation, are safe to handle and little skill to process. Glass fibres, conversely, require high amounts of capital investment and machinery, a pure source of feedstock materials, and a highly trained work force to handle possibly hazardous materials [19].

All factors considered, natural fibres provide a compelling case for use in reinforcing plastic matrix composites, replacing traditional reinforcing fibres like glass fibre and various petroleum based fibres [14].

2.1.2 Hemp Fibre and Morphology

Hemp fibre (genus species *Cannabis Sativa L*) can be considered to be a good choice for reinforcing polymer matrix composites, due to its high stiffness, strength and aspect ratio [20]. It also has an extremely high fibre yield per unit density and is disease and pest resistant, providing for low environmental impact production methods [21].

Traditionally, hemp fibre has been used over many millennia in many forms such as rope, cloth, sails for the shipping industry and paper [22]. Since the industrial revolution, hemp cultivation became less desirable, as other fibres had become easily available (primarily jute, cotton, sisal), as well as the decline in wind powered sail ships brought on by the rise of steam powered ships.

Hemp's association with marijuana has also had a severe effect on its cultivation, by virtue of it appearing like the plant containing significant hallucinogen levels (Figure 2.1). In reality, the quantity of the hallucinogenic chemical, THC (delta-9-tetrahydrocannabinol) present in the industrial species of hemp is extremely low [23, 24 and 25]. Nevertheless, the stigma persisted and resulted in a widespread ban in the cultivation of hemp throughout the world. Only recently has the industrial form of hemp been allowed to be cultivated under strict conditions in certain countries [23].

Hemp fibres are built up into fibre bundles held together by various substances in the hemp stem. The hemp stem structure can be observed in Figure 2.2. The hemp stem consists of an open structured pith core, within a woody core known as the hurd, surrounded by an outer bark comprising of cambium, the bast (phloem) fibre, cortex and epidermis. Usually, the term 'hemp fibre' refers to the bast section of the hemp plant, one of the most useful parts of the hemp plant.



Figure 2.1- A comparison of the varieties of hemp plant. Left : industrial hemp, Right: medical/hallucinogenic hemp [26]

The bast is the fibrous component that gives the plant its strength and form [26]. Bast fibres account for approximately 30 percent of the stem volume while the balance is mainly taken up by the hurd. Bast fibres are found within the bast region of the stalk grouped within fibre bundles. They are long, stiff and have high specific strength. It is these fibres, as already mentioned, have been used for rope and textiles and have been found suitable to be used as reinforcement for composites. The hurd fibres, on the other hand, are weak, brittle and are more suitable for use as filler in the paper industry and as animal bedding.

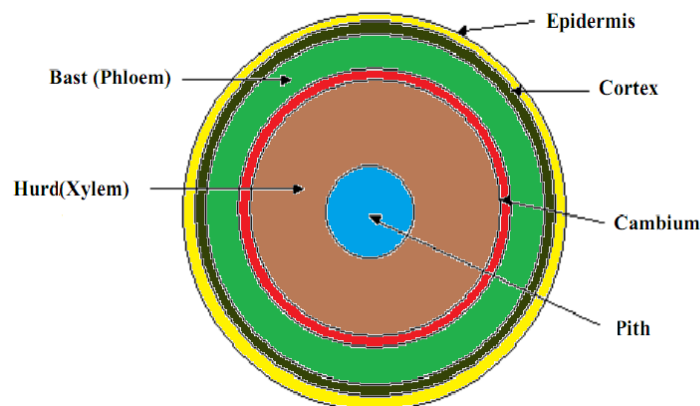


Figure 2.2 Schematic of hemp plant stalk [13]

The hemp bast fibres contain many of different chemical constituents and are themselves composites.

2.1.3 Hemp Fibre: its Chemical Constituents

Primarily, the hemp fibres consist of cellulose, hemicellulose, and lignin, with minute quantities of minerals, pectin, waxes and various water soluble components [27]. Hemp fibre consists of different constituents which vary in quantity based on cultivation density, quality of nutrients in the soil, and time of cultivation [28].

2.1.3.1 Cellulose

Cellulose gives bast fibres its strength and stiffness. It is built up of carbohydrate molecules; specifically, it is a polymer of saccharide units, consisting of D-anhydroglucophranose units bound with glycosidic bond linkages as depicted in Figure 2.3. In this figure, the bracketed part of the molecule represents cellulobiose, consisting of two anhydroglucose units. The arrangement of the polymerised molecules has been referred to as a chair structure, due to its alternating positioning of reactive groups [29].

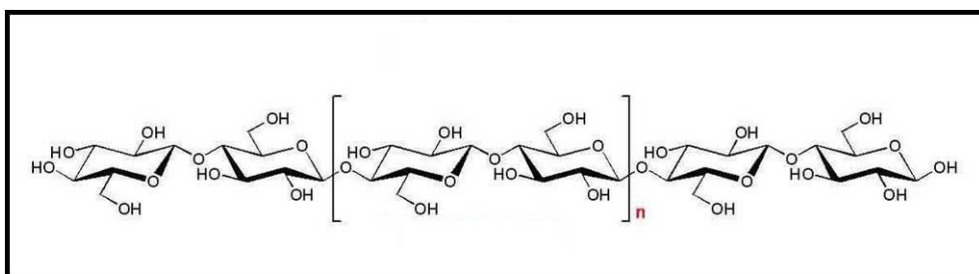


Figure 2.3 Chemical structure of cellulose [115]

Cellulose comprises of crystalline segments which make up to 80% of its structure [79] alternating with regions of amorphous cellulose [78] as shown in

Figure 2.4. However, it is the unencumbered inter-chain hydroxyl (OH) groups in its amorphous regions that leads to its hydrophilicity and that allow for hydrogen-bonding [30].

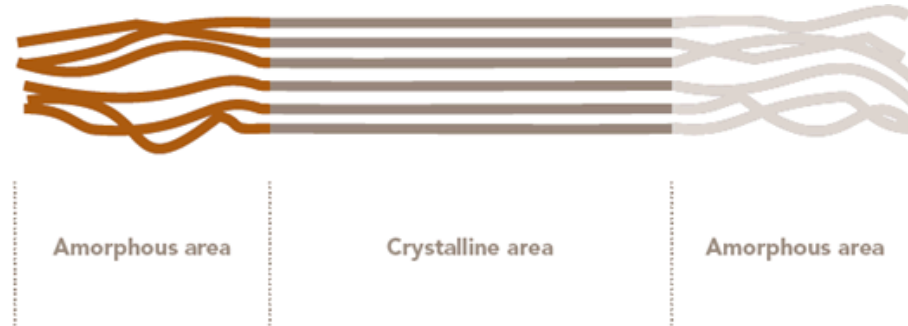


Figure 2.4 Schematic diagram of cellulose fibres [115]

2.1.3.2 Hemicelluloses

Hemicelluloses consist of polysaccharide polymers; they are often but not always homopolymers, which are composed of sugars like D-xylopyranose, D-glocopyranose, D-galactopyranose, L-arabinofuranose, D-mannopyranose, and D-glucopyranosyluronic acid with small quantities of other sugars [31]. Hemicellulose appears to bridge lignin and cellulose together, allowing for effective transfer of stresses between them [32]. Hemicellulose is mostly amorphous and is extremely hydrophilic due to its molecular structure being short and highly branched with short side chains of exposed hydroxyl (OH) groups (Figure 2.5).

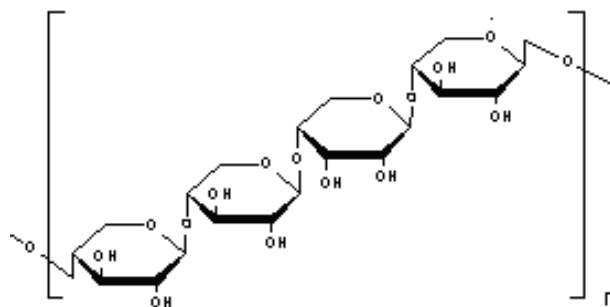


Figure 2.5 Hemicellulose molecular structures [116]

2.1.3.3 Lignin

Lignin is a complex aromatic polymer which is usually taken to be an adhesive that binds cell walls. Lignin is deposited in the wall during secondary wall synthesis and signals the end of cell expansion. Lignin occurs from the polymerisation of cinnamyl alcohols in three dimensions (Figure 2.6). Lignin is important to the plant, being one of the conductors of water transport in plant stems [33]. As the other materials in the plant are hydrophilic, lignin, which is a hydrophobic component, allows the transport of water throughout the plant's vascular system.

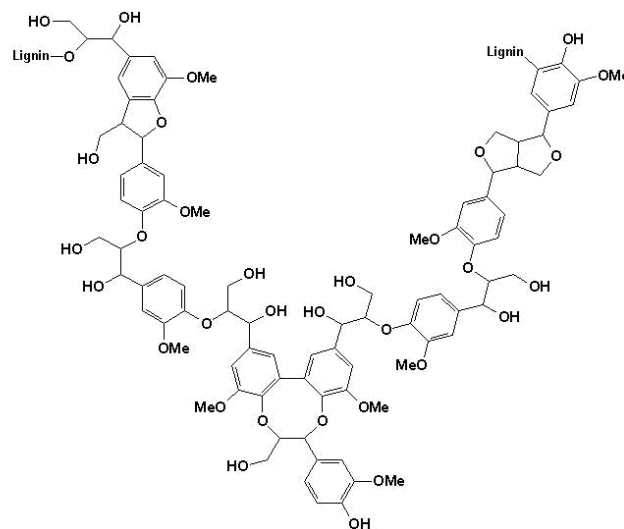


Figure 2.6 Lignin molecular structure [117]

2.1.3.4 Pectin

Pectin is the name for a group of sugars that include the polygalacturonosyl-containing polysaccharides and other polysaccharides that are covalently associated with them. Pectins perform a crucial role in holding the plant fibre structures together, along with lignin and hemicelluloses. Pectins are also extremely hydrophilic due to the incidence of carboxylic acid groups as well as

hydroxyl groups in the various sugars, allowing for hydrogen bonds to be formed [34]. Pectins can be considered long-chained composite structures illustrated in Figure 2.7.

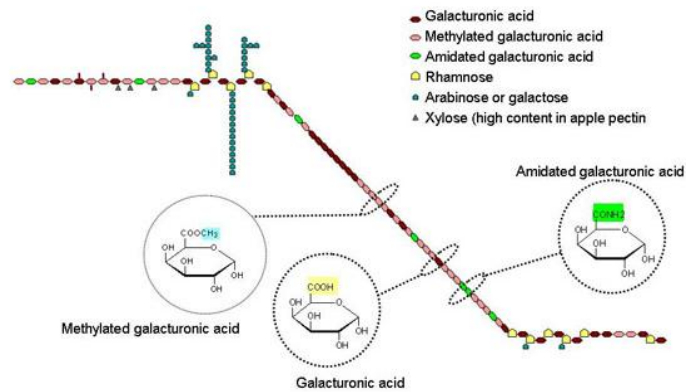


Figure 2.7 Pectin molecular and unitary arrangement [117]

2.1.4 Degradability of Hemp Fibre

Hemp fibre can be broken down into its base chemicals in several ways. The most beneficial way would be to utilise bacterium and noble rot to biologically “consume” the hemp fibre. Also, hemp can be degraded at very high temperatures without releasing adverse chemicals via hydrolysis. [35]

2.2 Bio-derived Thermoplastics

There are many types of bio-derived plastics that have been developed over the last hundred years including casein-based plastic and celluloid. Recently, the emphasis on the renewability and biodegradability of materials as emphasised by legislation and by customer demand, has led to the development of bio-plastics that are bio-derived and bio-degradable [36]. As such, there are several types of bio-plastics that are available and are being developed for commercial use.

Bio-plastics can be classified as plant-derived and animal-derived. Animal-derived bio-plastics are usually material that are considered to be waste products from the meat processing industry such as blood meal, and feathers. These bio-plastics are currently in their infancy and are being developed for commercial use [37].

Plant-derived bio-plastics are varied, but usually are derived from a carbohydrate source which is then fermented by bacteria and then processed into polymers. Among bio-degradable bio-plastics, three are currently available described below of which the first two have a certain amount of commercial success. They are:

- Poly(lactic acid) (PLA) – is a transparent plastic, which can be produced from corn sugar, cane sugar or any other sugar source. It resembles petroleum-derived plastics such as polyethylene (PE) or polypropylene (PP) in its characteristics. Also, it can also be processed using standard equipment that already exists for the production of conventional plastics. PLA normally comes in the form of granules, pellets or powder (each for specific uses) used in the packaging plastics industry for the production of various foils, moulds, tins, cups, bottles and other packaging [38].
- Starch based plastics – these plastics currently widely used in packaging for pharmaceutical industry and the food industry, for products such as plastic wrapping film and medicine delivery capsules [39]. Plasticisers such as sorbitol and glycerine are added so that starch can also be processed thermo-plastically. The characteristics of the material can be tailored to specific needs by varying the amounts of these additives.

- Poly-3-hydroxybutyrate (PHB) - The biopolymer poly-3-hydroxybutyrate (PHB) is a polyester produced by certain bacteria processing sugars or starch. Its characteristics are similar to those of the petroleum derived polypropylene. PHB can be produced as a transparent film with a melting point of higher than 130°C, and is biodegradable without residue. It is, however, very expensive to produce at the moment, limiting its uses [40].

Poly (lactic acid) (PLA) is then seen as a viable material for replacing petroleum-derived plastics due to its availability, its cost and its adaptability.

2.2.1 Poly (Lactic Acid) and its Sources

Poly(lactic Acid) or PLA, as previously mentioned, is a bio-derived polymer sourced from renewable resources, primarily being corn sugars. Other sources of raw material for the production of PLA include waste materials from agricultural activity [41]. PLA is a member of a group of aliphatic polyesters that are made from hydroxyl acids which are compostable and biodegradeable. PLA is obtained by fermenting the base feedstock with bacteria, producing lactic acid, the main monomer for PLA. Simply, two monomers of lactic acid combine to form lactides and these lactides polymerise to form PLA (Figure 2.8).

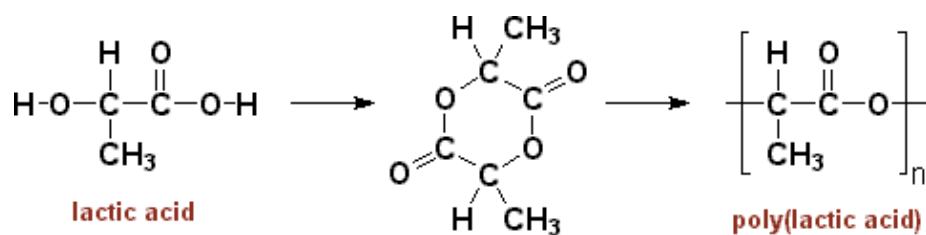


Figure 2.8 PLA monomer and polymerisation [118]

In actual fact, the nature of lactic acid is that it has stereo-isomers, L-lactic acid and D-lactic acid. Therefore, it can form three potential types of lactides: D-lactide, L-lactide and meso lactide. These structures are shown in Figure 2.9. Different types of PLA grades are obtained when different stereo isomeric structures of lactides are used in different compositions.

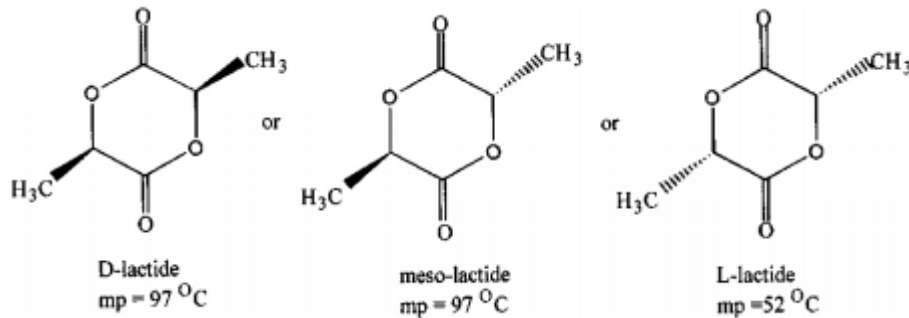


Figure 2.9 Stereo-isomeric structures of lactide [119]

As illustrated by Figure 2.10 [42], PLA production involves several steps from its base monomer, lactic acid, before it can be polymerised. Natureworks LLC developed a continuous process for the production of PLA from lactic acid. The process starts with a continuous condensation reaction (oligomerization) of aqueous lactic acid to produce a low molecular weight PLA pre-polymer. This pre-polymer then goes through a catalysed dimerization to form a cyclic intermediate dimer, known as lactide, which is then distilled to remove water. Then, the purified lactide is polymerised in a solvent-free ring opening polymerisation process and is processed into PLA pellets or powder which can then be sent out to customers who would then process the PLA into final components and products. At the end of the product's lifecycle, it can then be sent to an industrial recycling centre where it then recycled into compost or sent into a landfill for disposal [43].

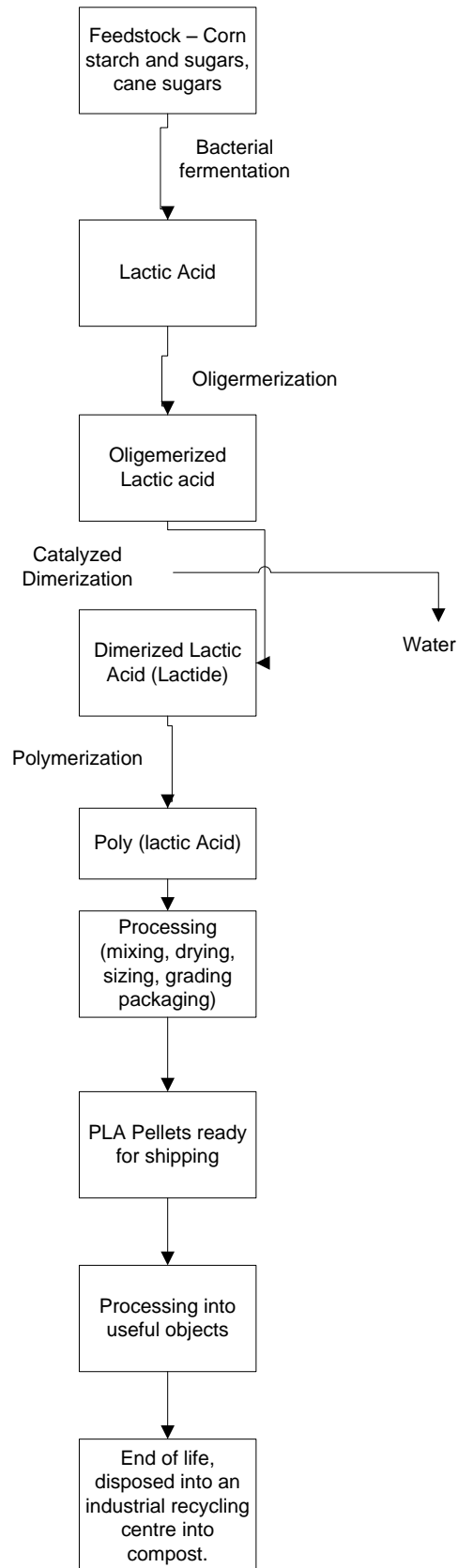


Figure 2.10 - Poly (lactic Acid) flow chart; from cradle to grave [44]

2.2.2 The Biodegradability of PLA

PLA can be considered a compostable, biodegradeable and hydrolysable material. It can decompose in any condition, as long as there is sufficient oxygen and water. It undergoes oxidative, hydrolytic and thermal degradation at high temperatures, so it is possible to break PLA down to its basic molecule which is lactic acid. This enables the material either to be safely disposed of or to be reused as feedstock for new PLA plastic production. [44]

2.3 Issues with use of Cellulose-based Natural Fibres in Bio-derived Matrix Composites

2.3.1 Cellulose-based Natural Fibres and its Issues

Natural fibre, being an organic material, has limitations associated with its durability under certain conditions [45] which severely affect overall material performance. These limitations relate to the following:

- Moisture absorption – fibres are hygroscopic
- Poor pest resistance, leading to rot and mould
- Thermal degradation at elevated temperatures
- Irregularities/defect within fibre structure
- Fibre damage while processing

Most of these issues can be overcome by treating the fibres to remove lignin as well as pectin and waxes [46], adding additive chemicals to chemically bond with the fibres to create a more uniform surface [47] and the use of use different processing methods in order to overcome the aforementioned limitations. Thermal resistance can be improved by using additives or fixatives to prevent excessive thermal degradation [48].

Hemp fibre by its very nature is variable; each batch that is received and stored will have different properties. The quantities of non cellulosic material in each batch would vary and as a result change the crystallinity values, material properties and change the way the fibre interfaces with the matrix. Short fibres are also a variable as their short length increases the propensity for it to be bunched up in one section of an extruder, making uneven fibre mix a major issue.

2.3.2 Bio-derived Matrices and their Issues

Bio-derived matrices include PLA, starch plastics and PHB. By nature these materials are delicate and require special handling methods [49]. There are several fundamental issues that affect the viability of these materials as feedstock for bio-plastics. Generally, they comprise of several traits:

- Hygroscopicity –they degrade with prolonged exposure to moisture
- Thermal degradation at elevated temperatures
- Hydrolysis in the presence of moisture at elevated temperatures
- Cross-linking caused by elevated temperature while processing
- Brittle material properties due to crystallisation or poor bonding

These issues can be overcome by adding plasticizers, preservatives and other chemicals that form bonds with the matrix [50], closing up the reactive groups and by processing the materials within a narrow temperature range to avoid cross-linking [51].

2.3.3 Hemp/PLA Fibre Composites and their Issues

As with individual fibres and matrices, Hemp/PLA composites face critical issues when it is compounded. Hemp is hygroscopic and will draw

moisture from the atmosphere if it is not encapsulated wholly within the PLA matrix. [52]. Hemp fibres can be pre-treated to remove any material including lignin, hemicellulose, pectin and waxes that would prevent fibre-matrix adhesion prior to being compounded with the PLA matrix. Another issue would be the low temperature processing requirements to prevent fibre charring and degradation; this would result in high PLA melt viscosities, resulting in insufficient fibre wetting. This can be overcome by adding various plasticisers or utilising the addition of another polymer to reduce viscosities at a lower temperature, leading to better fibre wetting and lower incidences of fibre charring [53].

2.4 Process and Manufacture of Composites

2.4.1 Basic Processes of Preparing Composite Components

Natural fibres are rarely used in their native state for reinforcing polymer matrices [54]. Surfaces of the fibre are usually covered with lignin, hemicelluloses, pectin and waxes that block the matrix from forming bonds with cellulose, the major structural material of the fibre, therefore limiting interfacial adhesion. The matrix also has its limitations; PLA in particular being hydrophobic, makes poor contact with the fibre interface [55]. Thus, modification to both the fibres and/or matrices is often conducted in order to ensure a suitable level of interfacial bonding.

Most natural fibres are pre-treated by retting, where the superfluous components of the plant stem are decomposed for a determined period of time, resulting in separation of useful fibre from waste material [56]. However, further processing treatments, mainly chemical treatments, are commonly used. Fibres are treated with chemicals to remove lignin, add functional groups and roughen the

fibre surface in order to maximise interfacial bonding between matrix and fibre [57]. Common among these chemical treatments include alkali treatment, acetylation and silane treatment,

2.4.1.1 Alkali treatments

Treating fibres with sodium hydroxide (NaOH) or NaOH and sodium sulphite (Na_2SO_3) combinations, at elevated temperatures, results in the removal and degradation of hemicelluloses, lignin, pectin and waxes. The removal of these materials allows the reactive hydroxyl (OH) groups on cellulose to be exposed, allowing effective bonding between matrix and fibre or coupling agent. This debonding also allows fibrils to be released from their fibre bundles, increasing the surface area for interfacial bonding with the matrix material [58].

2.4.1.2 Acetylation

Acetic anhydride ($(\text{CH}_3\text{CO})_2\text{O}$) is used to reduce the hydrophilic tendencies of cellulose fibres as well as allowing better fibre dispersion in a thermoplastic composite. It is a compatibilizer that forms acetate bonds with the reactive OH groups on the fibre surface, making them non-reactive and thus reducing the occurrence of OH bonding [59].

2.4.1.3 Silane treatments

Silane coupling agents have been used to perform as a bridge between reinforcing fibres and matrix material, usually for use with glass fibre. It promotes the interface binding of fibre and matrix in various other fibres as well. Silane coupling agents are compounds that are based on a silicon atom with differing and

customisable organic groups attached to it to suit different matrices and are hydrophilic. For natural fibre reactions, the process is complex, involving hydrolysis of certain organic groups to create hydrogen bonds [60].

Other fibre treatments have also been explored, such as bleaching, but they can damage the fibre [120]. Studies show that fibre surfaces can be altered by treatment and promote better fibre-matrix interfacing which lead to better composite properties.

2.4.1.4 Matrix treatments

Matrix modification can be used to optimise matrix-fibre interfacial bonding. Plasticisers may be added to increase the melt flow characteristics by reducing viscosity of the polymer melt in order for it to provide sufficient fibre wetting at lower processing temperatures, which is to prevent fibre charring. Improving melt flow also increases matrix-fibre compatibility. In some applications, different types of polymers may be mixed in order to achieve a similar effect [61]

2.4.2 Basic Manufacture of Composites

Manufacture of composites can be split into two parts: mixing and shaping. Mixing natural reinforcing fibres and polymer matrices together is an important process to ensure good fibre dispersion and good fibre-matrix interfacing. The most common mixing process methods are melt mixing and extrusion; while injection moulding and compression moulding are the common methods for forming complex composite objects.

2.4.2.1 Melt mixing

Melt mixing using a radial turbulent flow mixer is a commonly used method for compounding short reinforcing fibres with thermoplastic polymers in small batches. The polymer is first heated up in a chamber with a continuously rotating impeller. Once the polymer has reached a suitable viscosity, reinforcement fibres are added into the melt. The final composite melt mix can be formed into whatever form desired after it is evenly mixed but that requires a further processing stage. Although melt mixing allows for very good mixing of fibre with polymer, its efficacy is limited by the characteristic of being a batch-based process at a time. This results in repeated machine shutdowns as the melt mix needs to be taken out of the mixer in order for the next batch to be processed. Another main issue would be the incidence of fibre breakage and degradation with long mixing times, high mixing speeds and melt temperatures that are either too high or too low [62].

2.4.2.2 Extrusion

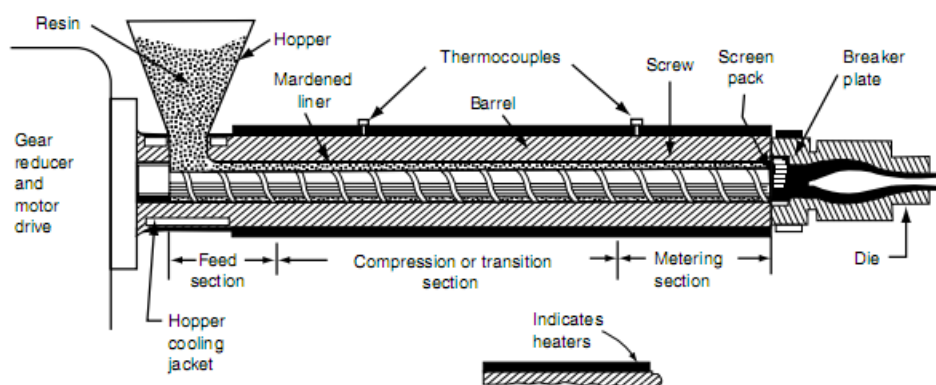


Figure 2.11 The Extruder

Extrusion is a very efficacious method of compounding natural fibres and thermoplastic polymers. Thermoplastic polymers, in a pellet or powder form and short chopped reinforcing fibres are mixed and are forced into a heated extrusion barrel by means of one or two co-rotating screws. The polymer is then melted and mixed with the fibres to form a composite melt, which is then drawn through the extruder barrel, whilst undergoing further mixing and is compressed to improve the uniformity of melt mix. The extruder melt mix is then forced out of the barrel through a shaped die. Figure 2.11 illustrates the typical configuration of an extruder.

Extrusion is often carried out before final moulding because excellent fibre distribution can be achieved within the polymer matrix in extrusion. The extruded composite is then granulated or ground into pellets that are easily injection moulded into other complex shapes. It is necessary to optimise the extruder processing variables, such as barrel length, temperature profile, back pressure, screw configuration and screw speed in order to produce composites with optimal mechanical properties and fibre distribution. If the variables are less than ideal, excessive fibre shortening, fibre damage, poor fibre dispersion and poor fibre wetting can occur. Fibre damage usually occurs due to the crushing screw action, fibre-fibre friction, polymer-fibre friction and incorrect processing temperatures [63]. Fibre breakage can be reduced drastically by separating the feed for fibres and matrices; excessively high fibre shear forces and insufficient fibre wetting can be avoided by configuring the machine so that the polymer melts first and then to introduce the fibres after the polymer melt is fully melted further in the barrel. Also, by utilising an extruder with a shorter barrel and screw, the length of fibres can be preserved as the shorter residence duration and the less

number of mixing elements (turns on the screw) can reduce the chance of breakage [64]. The processing temperature is another crucial component to fibre/polymer compounding. The polymer matrix will be too viscous to flow around the fibres if temperature is too low, resulting in poor fibre wetting leading to a weaker composite. On the other hand, degradation of fibres and polymer will occur if the processing temperatures are too high; again resulting in reductions in composite strength [65].

Extrusion is a continuous process that is capable of high feed rates which allows for quick and efficient processing of materials. In addition to mixing, extruders can be used to make various continuous length products through the use of specifically shaped dies.

2.4.2.3 Injection Moulding

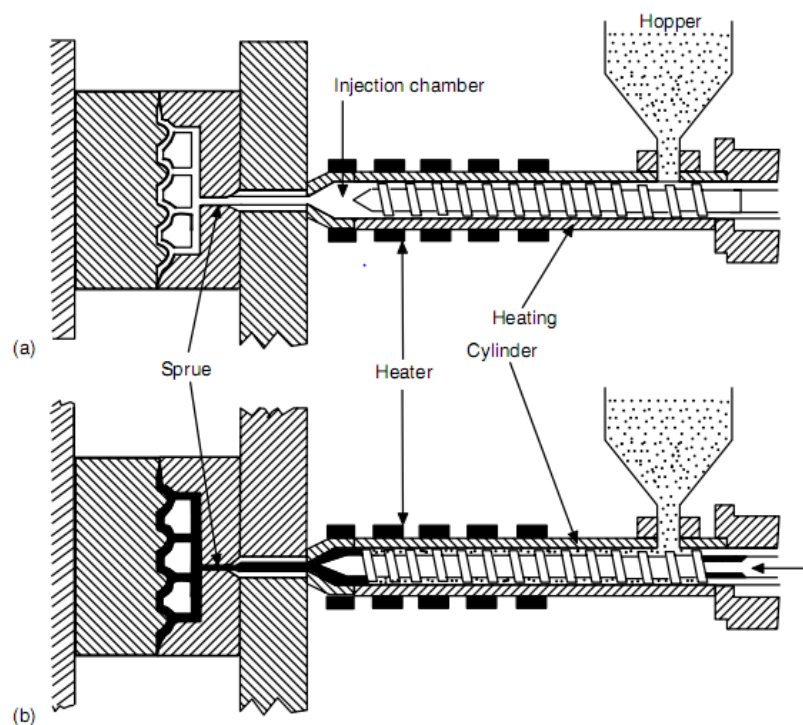


Figure 2.12 Injection Moulding, (a) loading melt chamber (b) inject material into mould

Injection moulding is among the most widely used processes for manufacturing moulded parts using thermoplastic and fibre-reinforced thermoplastic materials (Figure 2.12). It is a high production rate manufacturing process capable of producing shaped composite parts in high volumes. Short fibre reinforced composites can be processed into complex shaped components using standard thermoplastic injection moulding equipment [67]. When used in injection moulding applications, composite materials must be capable of fluid-like flow; as a result, they usually consist of short fibres with a relatively low fibre fraction which is usually less than fifty percent of weight fraction of end composite or less than thirty percent of fibre by volume. This is a crucial criteria which needs to be considered carefully, as low fibre content can result in insufficient matrix reinforcement, and excessively high fibre content can lead to poor moulding and reduced mechanical properties of the composite [68].

Injection moulding is a crucial step, many variables involved in it. They are the mould cooling temperatures, mould residence times and material back pressure. Mould cooling temperatures influences the final crystallinity of the material, as would the residence time. Material back pressure determines what pressures the injection of melt material takes place at, too low pressures would result in insufficient filling of mould and a too high rate would result in uneven quantities of fibre. This pressure also induces the fibres in the composite melt mix to align themselves according to the contours of the mould.

A heating element is added to the mould cooling system in order to get an even cooling period for the specimens and an optimal back pressure is selected before moulding.

The injection moulder melts pre-formed short fibre reinforced composite granules in a screw driven barrel, sending composite melt to the machine nozzle. It then injects a measured amount of melt into the mould. The mould unit, which has two sections, a moving and a stationary section, encapsulates the injected composite within its form in which is cooled, creating a final component. Injection moulding can be used to induce a certain degree of fibre alignment and reduce fibre damage, resulting in a better reinforced final component [69] compared to other methods of forming.

2.4.2.4 Compression Moulding

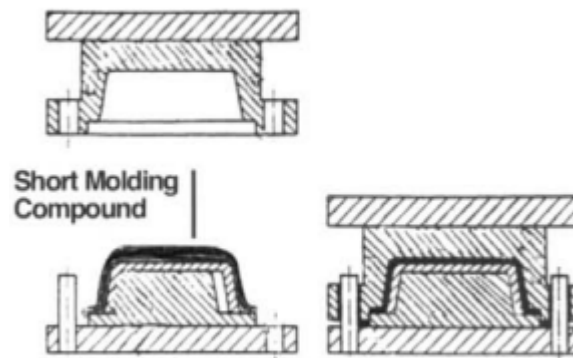


Figure 2.13 Compression mould schematic diagram

Compression moulding is a common method of production by which many types of plastics can be processed, as well as composites with long continuous fibre reinforcement mats. It is a process used in various industries to fabricate simple and large components, notably in the automotive industry for large laminated parts, such as the dashboard [70]. The manufacture of composite fibre material using this process involves a press with heated platens (for sheets) or heated moulds (for complex components). A two part mould is used as per Figure

2.13, and the fibres and matrix material (in powder, granule or sheet form) are laid alternately within the bottom half of the mould. Alternatively, premixed short fibre composite granules could be used. The two halves of the mould are preheated and are closed together, allowing the matrix material to infiltrate the fibre layers under pressure while forcing the air out of the fibre layers. The whole component is held for a cooling period to ensure that the entire fibre structure has been well consolidated with the matrix material, after which it is released and the composite component removed from the mould [71].

2.4.3 Process and Manufacture of Hemp/PLA Fibre

The processing of hemp/PLA composites is similar to that of other thermoplastic matrix/short fibre composites, with special care to be taken in consideration of PLA's propensity to hydrolyse in the presence of moisture [72]. Thus, precautions must be taken to ensure that during the compounding step, the hemp fibre to be used must be dry as well as free of loose particles that may compromise the final material's properties.

Processing temperatures and feed rates are also important with regards to fibre damage and material degradation. When hemp/PLA is processed for extended periods of time at elevated temperatures, both the fibre and polymer matrix undergo chemical degradation resulting in poor composites. On the other hand, when temperatures are below ideal, the melt will become less viscous and would result in fibre damage due to matrix material shear forces.

Processing of hemp/PLA composites is best carried out using extrusion followed by injection moulding to form the final specimen. This allows for the

shortest residence times in the machines at elevated temperatures leading to less fibre and matrix degradation.

Heat treatment or “annealing” can be used in order to affect the molecular structure of a polymer material. However, there are various vagaries involved with annealing. Annealing which takes place in an oven could mean that the heat introduced would not affect the specimens evenly, as the matrix and fibres are relatively poor heat conductors. A forced convection oven could be used to ensure that the heat flow over the specimens is even.

2.5 Crystallinity of Polymers and Composite materials.

2.5.1 Crystallinity of Polymers

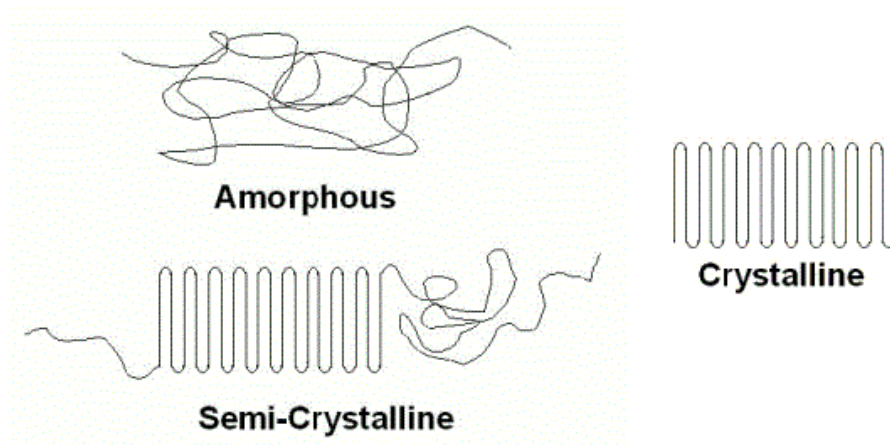


Figure 2.14 Schematic diagram of polymer chain alignments

Crystallinity occurs in many thermoplastic polymers; it is a phenomenon where segments within the polymer chain either align themselves in an orderly, structured fashion or align themselves with portions of adjacent polymer chains in a similar manner (Figure 2.14). Crystallinity tends to improve properties such as strength and impact resistance [73]. Crystallinity does not exist when the polymer melt is above the melt temperature. As the polymer temperature drops below the

melt temperature, crystallinity begins to form. The faster the polymer cools, the less the degree of crystallinity [74]. The presence of crystallinity induces the linearity of crack propagation paths in a polymeric material due to the increased incidence of crystal spherulites which would make the stress concentration focused along the arrangement of crystals [75]. Crystallinity also increases the thermal stability of polymers due to the coordination of secondary bonds between polymer chains which occurs within crystalline region. This leads to the polymer requiring higher amounts of energy input in order to break cross-linkages in the polymer structure [76]. In some DMTA studies, it has been found that crystallinity leads to values of storage modulus of a material being relatively stable all throughout the temperature testing range, right up to its melting point, as the material's elasticity would only drop very slightly, much less compared to for less crystalline material [77].

2.5.2 Crystallinity in PLA and its Composites

Crystallinity in PLA is influenced by many factors. The relative amounts of L-Lactide acid to D-Lactide acid determine the propensity of crystal spherulites to form within the matrix bulk [80]. The incidence of D-Lactide acid in PLA polymer mix induces crystallisation and results in a crystalline form of PLA [81].

Hemp fibre surfaces can serve as nucleating surfaces where crystalline structures in the matrix can be induced [82].

2.6 Physical and Mechanical Characterisation Methods

There are various methods used to analyse composite materials with regards to its material properties; the ones of interest are physical and mechanical characterisation. Most mechanical characterisation methods are destructive, for

example, single edge notch bending (SENB) fracture toughness testing, tensile testing, and differential scanning calorimetry. There are also other non destructive mechanical characterisation tests that can be carried out to analyse the composite material. Dynamic Mechanical Thermal Analysis is one non-destructive test that can be carried out on specimens to determine the various material properties that change with the variation of ambient temperature [84].

Physical characterisation methods such as polarised optical microscopy and scanning electron microscopy (SEM) are methods to analyse effects of these destructive tests on the material specimen. X-ray diffraction has been used to characterise the compositions of natural fibres as well as determine its crystallinity, due to the presence of crystalline cellulose [83]. It can also be used to detect crystalline structures in the matrix material of the composite.

Chapter 3: Materials and Methods

3.1 Experimental Overview

The purpose of this research is to assess the potential to control crystallinity and the influence of crystallinity on composite properties. To achieve this objective, hemp fibres were chemically treated with alkali to remove lignin, thus improving the fibre strength, improve fibre separation and to modify the fibre surface.

Composites were produced by compounding chopped fibres and PLA pellets in a twin-screw extruder, and the extruded composites were then granulated and injection moulding into test specimens.

The resulting specimens were put into an oven and were annealed at different temperatures for varying time periods. The resulting composite specimens were analysed to evaluate various physical attributes, such as strength, Young's modulus, crystallinity and thermal stability.

3.2 Materials Used

Specific materials were chosen for their suitability to match certain criteria, namely their biodegradability and best fit for certain processing methods. Poly(lactic acid) (PLA) was used because it was easily utilised in existing plastics processing and production machines as well as its ease of availability [85]. Also, the availability and strength of the materials was taken into consideration. Therefore, hemp fibre was chosen to be the reinforcing fibre because of its strength as well as its availability.

3.2.1 Hemp Fibre and its Treatment

Retted industrial hemp fibre (*Cannabis Sativa L.*), supplied by Hemcore (UK), was treated with a 5 wt% solution of NaOH at 50°C for 1 hour, such that the fibre: liquor ratio was 1:5 (by weigh). The average fibre length was 3.65mm. In order to treat a 70g sample of hemp fibre with the required alkali solution concentration and fibre: liquor ratio, 42g of analytical grade NaOH (98% purity) was dissolved in 378ml water and added to the pre-weighed fibre. This particular treatment was found to be the optimal for improving the tensile strength and fibre separation of hemp [86]. The fibre was then washed in warm flowing water at 50°C for 30 minutes and placed in an oven to dry for approximately 48 hours at 60°C.

3.2.2 Poly(lactic acid) (PLA)

PLA polymer 4042D, from NatureWorks LLC, USA, via Convex Plastics was used as a matrix material. The PLA was provided in pellet form and its density was 1.25 g/cc. The PLA pellets were placed in an oven to dry for approximately 48 hours at 60°C, before being compounded with hemp fibre.

3.3 Fabrication of Composites

Hemp/PLA fibre composites were compounded (0%, 15% and 30 wt% fibre) in a ThermoPrism TSE-16-TC twin screw extruder.



Figure 3.1 Fibre/PLA mix prior to compounding in extruder



Figure 3.2 Fibre/PLA mix being fed down the extruder's hopper



Figure 3.3: Extruder where composite is compounded



Figure 3.4 compounded Hemp/PLA extrude prior to being granulated

The extruded composite material was then pelletised in a granulator, dried at 80°C for 24 hours and then injection moulded into standard fracture toughness test pieces using a BOY15-S injection moulding machine, with the mould being kept at room temperature.



Figure 3.5 Boy15-S Injection moulding machine



Figure 3.6 Some of the fracture toughness testing samples,

Single Fibre thin samples were made by placing glass slips on a heating plate, heating it to approximately 180°C and placing a tiny chip of PLA on its surface. Once it had melted, a fibre that had been separated from a hemp fibre bundle was placed on the melted PLA chip and then was sandwiched with another glass slip and then pressed down hard until it is thin, as illustrated in Figure 3.7. They were then placed in an oven at 100°C for 30 minutes.

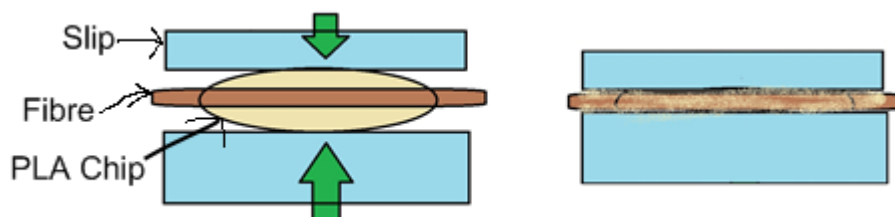


Figure 3.7 Left: Glass slip-slide prior to being pressed Right: After pressing

3.4 Treatment of Fabricated Composites

The completed composites were then annealed at 70°C and 100°C for 3 hours, 8 hours and 24 hours in an oven (Table 3.1).

Table 3.1 Schedule of treatments for various Matrix/fibre combinations

PLA						
	70°C			100°C		
control	3hr	8hrs	24hrs	3hr	8hrs	24hrs
15 wt% hemp/PLA						
	70°C			100°C		
Control	3hr	8hrs	24hrs	3hr	8hrs	24hrs
30 wt% hemp/PLA						
	70°C			100°C		
Control	3hr	8hrs	24hrs	3hr	8hrs	24hrs

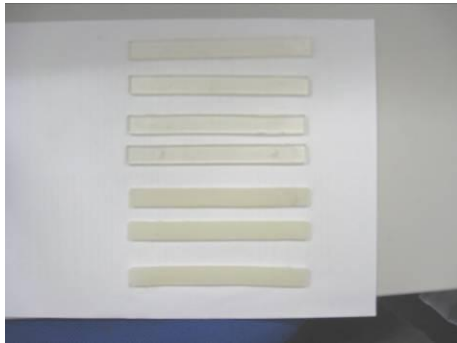


Figure 3.8 Samples of PLA, in order from the top: control sample, annealed at 70°C for 3hrs, 70°C 8hrs, 70°C 24hrs, 100°C 3hrs, 100°C 8hrs, 100°C 24hrs



Figure 3.9 Samples of 15 wt% hemp /PLA left to right - control sample, annealed at 70°C for 3hrs, 70°C 8hrs, 70°C 24hrs, 100°C 3hrs, 100°C 8hrs, 100°C 24hrs



Figure 3.10 Samples of 30 wt% hemp /PLA left to right - control sample, annealed at 70°C for 3hrs, 70°C 8hrs, 70°C 24hrs, 100°C 3hrs, 100°C 8hrs, 100°C 24hrs

3.5 Analysis of Composites

3.5.1 Scanning Electron Microscope (SEM)

In this study, fibre surface topography and composite fracture surface morphology was studied using Hitachi S-4000 and S-4700 field emission scanning electron microscopes. All samples were ion sputter-coated with platinum and palladium to provide enhanced conductivity. Samples were mounted with carbon tape on aluminium stubs and then sputter coated with platinum and palladium to make them conductive prior to SEM observation.



Figure 3.11 The SEM



Figure 3.12 Aluminium stubs with mounted platinum/ palladium sputtered test pieces

3.5.2 Differential Scanning Calorimetry (DSC)

The thermal behaviour of PLA and its composites was assessed using a DSC 2920-TA Instruments machine. All DSC scans were carried out at a scan rate of 10°C/min from room temperature to 200°C in the presence of air using samples of approximately 8-10mg. The percentage crystallinity (X_{DSC}) has calculated using the following equation [90].

$$X_{DSC}(\%) = \frac{\Delta H_f - \Delta H_{CC}}{\Delta H_f^o} \times \frac{100}{w}$$

where $\Delta H_f^o = 93 \text{ J/g}$ for 100% crystalline PLA, ΔH_f is the enthalpy of melting, ΔH_{cc} is the cold crystallisation enthalpy and w is the weight fraction of the composite.



Figure 3.13 Differential scanning calorimetry machine

3.5.3 X-Ray Diffraction Analysis (XRD)

A Philips X-ray diffractometer, employing $\text{CuK}\alpha$ radiation of wavelength, $\lambda = 1.54$ and a graphite monochromator with a current of 40 mA and a voltage of 40 mV was used to evaluate the composite specimen. The diffraction intensity was in the range of 12° to 45° of 2θ (Bragg angle), and the scanning speed was $0.03^\circ/\text{sec}$. XRD analysis allows for a simple method to calculate the crystallinity index of its cellulose fibre materials by means of the empirical Segal equation [92, 96] which is as follows:-

$$I_{\text{XRD}} = \frac{I_{002} - I_{\text{amp}}}{I_{002}} \times 100\%$$

where I_{XRD} crystallinity index, I_{002} is the maximum intensity of the 002 lattice diffraction plane at an angle 2θ of between 22° and 23° and I_{amp} is the diffraction intensity at an angle 2θ close to 18° representing amorphous materials in cellulosic fibres.

3.5.4 Polarised Optical Microscope (POM)

Fracture profiles and surfaces of the specimens were analysed using an Olympus BX60F5 optical light microscope, utilising the built in polarising filters and micrographs were taken using an attached Nikon Digital Sight DS-U1 Camera. Single fibre/PLA glass slide samples were examined as well.

Other photographs of equipment and samples were taken using a 3.2 megapixel camera on a Sony Ericsson P1i mobile digital assistant.

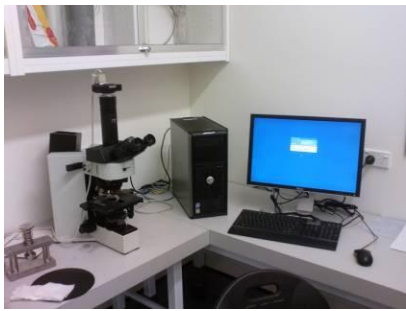


Figure 3.14 Polarised Optical Microscope setup

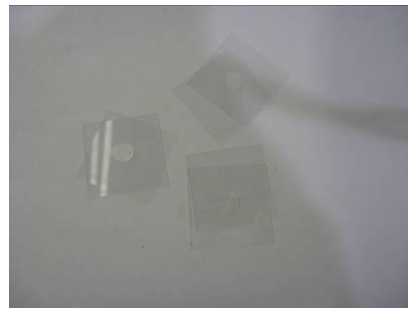


Figure 3.15 Single fibre/PLA glass slide samples

3.5.5 Fracture toughness (K_{1C}) and tensile testing

Mode I fracture toughness testing was carried out using single-edge-notched bend (SENB) specimens according to the ASTM D 5045-99 Standard Test Methods for Plane-Strain Fracture Toughness and Strain Energy Release Rate of Plastic Materials [88]. The length (L), span length (S), width (W) and thickness (B) of the specimens were 126, 56, 12.7 (± 0.03) and 3.5 (± 0.03) mm respectively, which satisfies the condition of $2B < W < 4B$ as specified in the standard. The initial crack length (a) was 6.35 mm (± 0.005). The loading speed was 2 mm/min and 10 mm/min and the notch root of the specimens was sharpened using a razor blade before testing. Five specimens were tested for each

batch of composite in a Lloyd LR 100k Universal Testing machine. Specimen configuration is shown in Figure 3.16 and 3.17.



Figure 3.16 Fracture toughness sample with notch

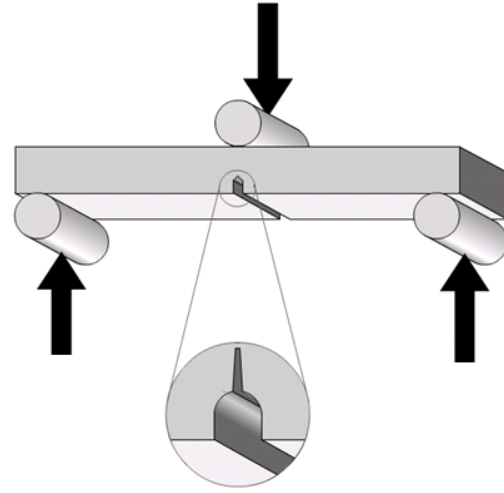


Figure 3.17 Diagram representing a 3 point Single End Notch Bending fracture toughness configuration.

Critical stress intensity factor, (K_{IC}) of SENB specimens can be calculated using the following relations [88]:

$$K_Q = \left(\frac{P_Q}{BW^{1/2}} \right) f(x)$$

Where K_Q is trial K_{IC} , and $0 < x < 1$.

$$f(x) = 6x^{1/2} \frac{[1.99 - x(1-x)(2.15 - 2.93x + 2.7x^2)]}{(1+2x)(1-x)^{3/2}}$$

where P_Q is the load, $f(x)$ is the geometrical correction expressed as a/W , and the a is the initial crack length. P_Q can be measured from the load versus deformation curve.

batch of composite in a Lloyd LR 100k Universal Testing machine. Specimen configuration is shown in Figure 3.16 and 3.17.



Figure 3.16 Fracture toughness sample with notch

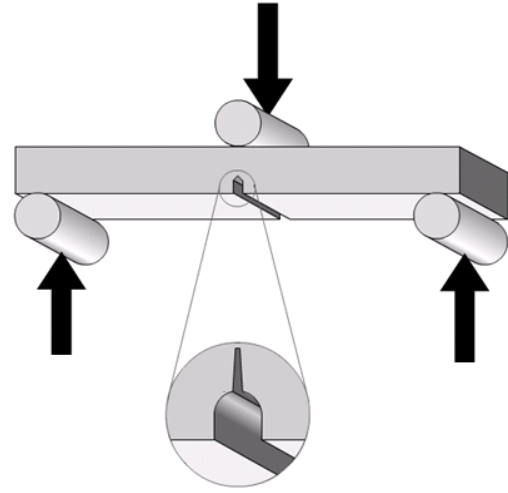


Figure 3.17 Diagram representing a 3 point Single End Notch Bending fracture toughness configuration.

Critical stress intensity factor, (K_{IC}) of SENB specimens can be calculated using the following relations [88]:

$$K_Q = \left(\frac{P_Q}{BW^{1/2}} \right) f(x)$$

Where K_Q is trial K_{IC} , and $0 < x < 1$.

$$f(x) = 6x^{1/2} \frac{[1.99 - x(1-x)(2.15 - 3.93x + 2.7x^2)]}{(1+2x)(1-x)^{3/2}}$$

where P_Q is the load, x is the geometrical correction expressed as a/W . P_Q can be measured from the load versus deformation curve.

For the K_Q values to be accepted as K_{IC} , the following formula must be satisfied

$$B, a, (W - a) > 2.5(K_Q / \sigma_y)^2$$

And thus,

$$K_{IC} = K_Q$$

Tensile testing

Tensile testing was carried out according to the ASTM D 638-03 Standard Test Method for Tensile Properties of Plastics [89]. Samples were tested using an Instron 4042 universal testing machine fitted for tensile testing with a 50 kN-load cell. The cross-head speeds were 2 mm/min and 10 mm/min. Load versus extension data were acquired by computer, which also facilitated machine control. Strain was measured with an extensometer, attached to the central portion of the test specimen with clips. Five samples were evaluated for each batch of samples.



Figure 3.18 Tensile testing samples



Figure 3.19 Instron universal testing machine for tensile testing

3.5.4 Dynamic Mechanical Thermal Analysis (DMTA)

DMTA is a non-destructive testing method that involves the application of an oscillating force on a test specimen, which results in a sinusoidal stress being applied to it, resulting in sinusoidal strain. The sinusoidal strain curve lags behind that of stress, by a phase angle of δ . This makes the DMTA sensitive to

mechanical responses of a material which are tracked using various sensors, monitoring dynamic property changes as a function of frequency, temperature or time in a controlled environment [91]. In this study, the storage modulus (E') (resistance to deformation), loss modulus (E'') (tendency to flow) and the dissipation energy of cyclic loading/ damping ($\tan \delta$) (being the ratio of E'' to E' and is related to the degree of mobility of a material) were measured at the frequencies of 1 Hz and 10 Hz from room temperature to 130°C using a Perkin-Elmer DMTA 8000 analyser and a single end cantilever beam flexure bending testing fixture on the horizontal plane. The specimen dimensions were on average approximately 12.5x12.5x3.5 mm.

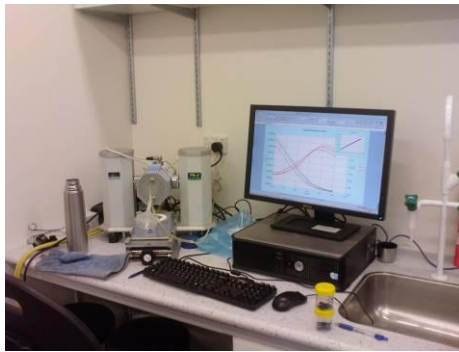


Figure 3.20 Dynamic mechanical analyser during a test run

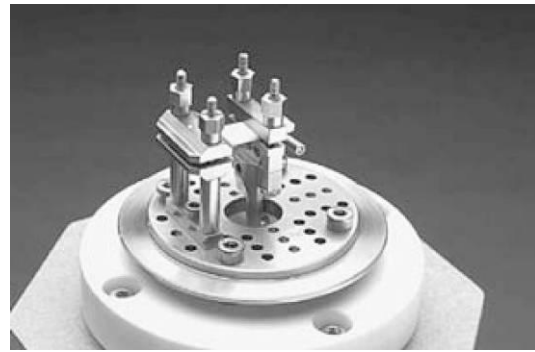


Figure 3.21 Dynamic mechanical analyser test apparatus set-up, single end cantilever.

Chapter 4: Results and Discussion

4.1 Introduction

The main aim of this research thesis was to study the possibility of controlling crystallinity in hemp/PLA composites by annealing samples at different temperatures for different durations and determining the effects of this treatment on material properties such as fracture toughness, tensile strength, and thermal stability.

The physical appearances of control and annealed samples for PLA and different fibre fractions can be observed in Figures, 4.1, 4.2 and 4.3. It was found that differences in translucence could be observed in PLA, primarily being clear in its control state and at the lower annealing temperature of 70°C and appearing opaque when the annealing temperature was 100°C. The appearance of composite samples did not differ vastly. However, upon closer observation, it can be discerned that the control samples and those annealed at 70°C for both 15 and 30 wt% hemp reinforced PLA composite were more translucent when compared to the samples annealed at 100°C.

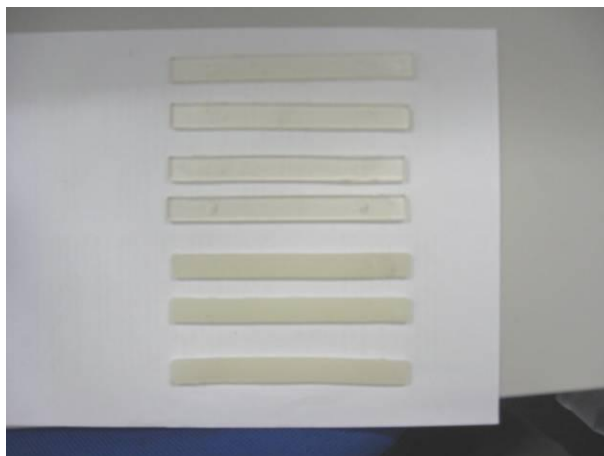


Figure 4.1 Annealed samples of PLA, in order from the top: Control sample, and annealed at 70°C 3hrs, 70°C 8hrs, 70°C 24hrs, 100°C 3hrs, 100°C 8hrs and 100°C 24hrs



Figure 4.2 15 wt% hemp/PLA left to right
Control sample, annealed at 70°C 3hrs,
70°C 8hrs, 70°C 24hr, 100°C 3hr, 100°C 8hr,
100°C 24h



Figure 4.3 30 wt% hemp/PLA left to right
Control sample, annealed at 70°C 3hrs, 70°C
8hrs, 70°C 24hrs, 100°C 3hrs, 100°C 8hrs,
100°C 24hrs

4.2 Experimental Results and Discussion

4.2.1 Scanning Electron Microscope (SEM) Analysis

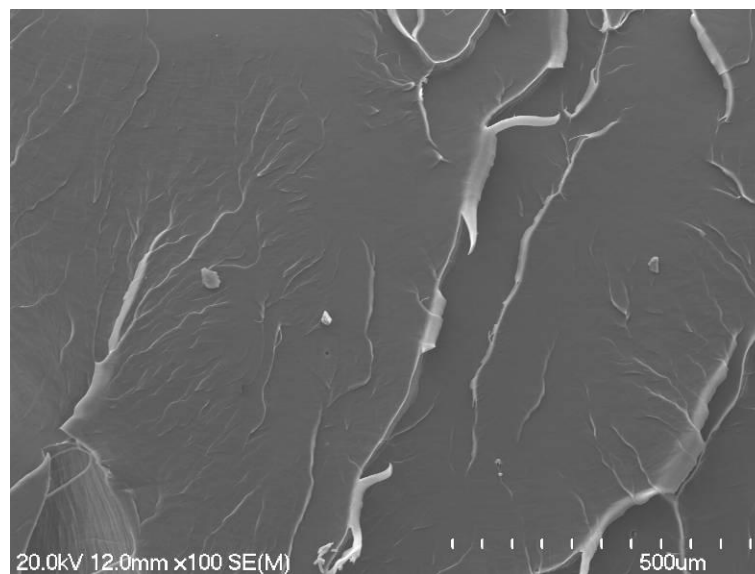


Figure 4.4 SEM of fracture surface of PLA control sample fracture toughness tested at 10mm/min

SEM analysis provides a clear look at the surface morphology of fracture surfaces. It was found that the fracture surface of the PLA control sample (Figure 4.4) was relatively smooth and flat, though it had some matrix deformation/tearing as seen from ridges formed. Thus, failure of PLA is largely brittle with some limited ductility

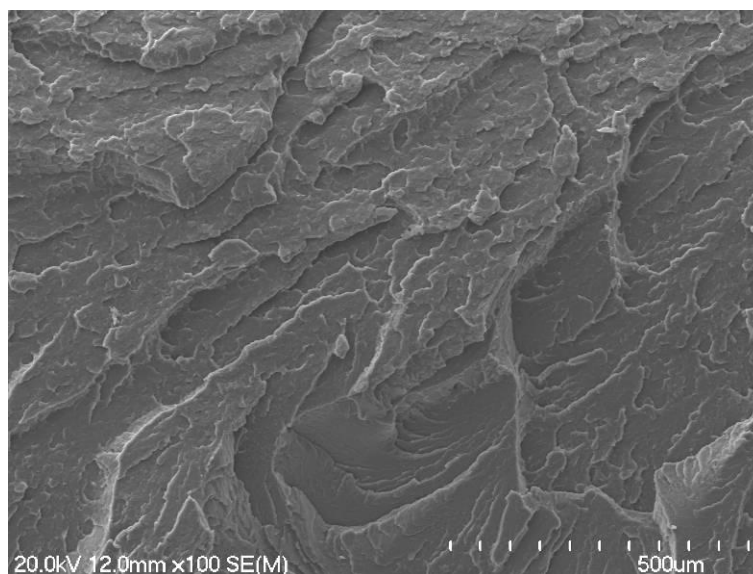


Figure 4.5 SEM of fracture surface of PLA 100°C 24hrs sample fracture toughness tested at 10mm/min

On the other hand, the fracture surfaces of PLA annealed at 100°C for 24 hrs (Figure 4.5) were rougher; appearing bumpy and mottled supporting the presence of crystallinity and that crystallinity was influencing fracture behaviour [93].

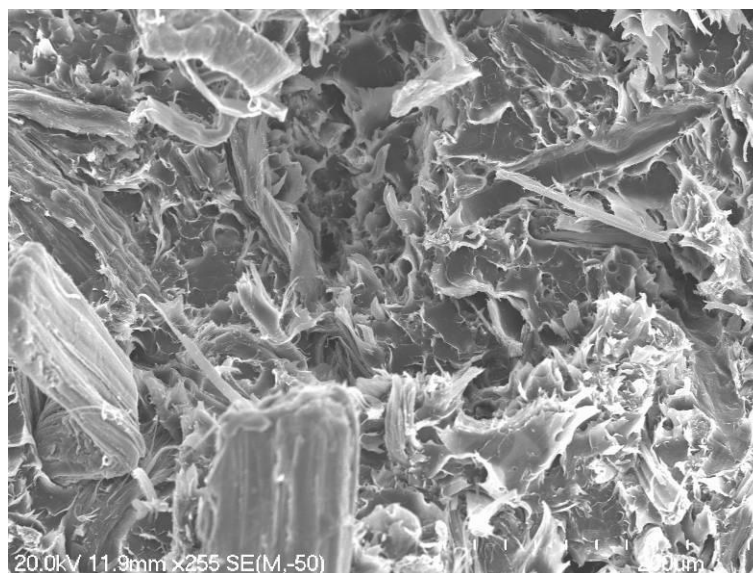


Figure 4.6 SEM of fracture surface of 15 wt% hemp/ PLA control sample fracture toughness tested at 10mm/min

Fibre pull-out and fibre fracture was observed in the 15 wt% hemp/ PLA control (Figure 4.6). Irregular arrangement of fibres was also observed, showing

that the process of injection moulding does not necessarily distribute fibres evenly along a test sample's length [94].

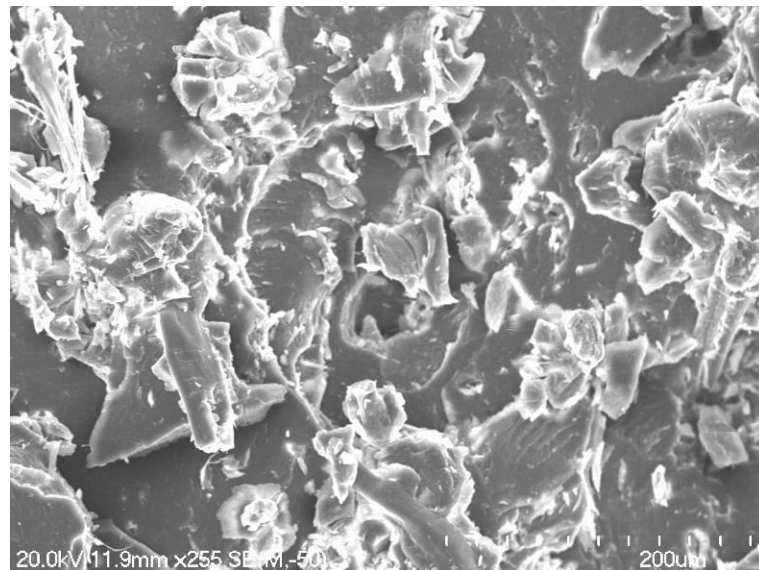


Figure 4.7 SEM of fracture surface of 15 wt% hemp/ PLA100°C 24hrs sample fracture toughness tested at 10mm/min

Figure 4.7 shows the fracture surface of 15 wt% hemp/ PLA annealed at 100°C for 24 hours sample where more fibre fracture appears to have occurred, suggesting more brittle behaviour.



Figure 4.8 SEM of fracture surface of 30 wt% hemp/ PLA control sample fracture toughness tested at 10mm/min

Figure 4.8 represents a micrograph of a 30 wt% hemp/ PLA control fracture surface (Figure 4.8) showing a fibre/fibril that has experienced pull-out, but with the notable difference being that it is a cleaner fibre/fibril pull-out when compared with Figure 4.6. Figure 4.8 has a higher fibre fraction, so one possibility is that there has been less matrix-fibre wetting [95]. Alternatively, the increased fibre content could be leading to increased stress concentration leading to more premature failure.

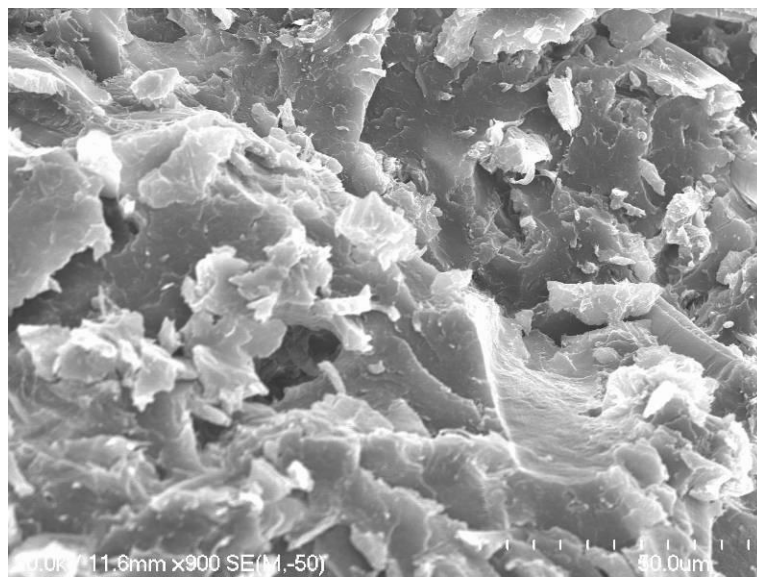


Figure 4.9 SEM of fracture surface of 30 wt% hemp/ PLA100°C 24hrs sample at 10mm/min

Figure 4.9 shows the fracture surface of a sample of PLA/30 wt % hemp annealed at 100°C for 24 hours, which differs vastly from the control sample (Figure 4.8) due to more visible fibre fracture and the lack of fibre pull-out.

SEM observations show that there is a distinct difference between unannealed and annealed samples' fracture surfaces. Elevated crystallinity and transcrystallinity on fibres are surmised to contribute to this difference in appearance.

Figure 4.8 represents a micrograph of a 30 wt% hemp/PLA control sample fracture surface showing a fibre/fibril that has experienced pull-out, but with the notable difference being that it is a cleaner fibre/fibril pull-out when compared to Figure 4.6. Figure 4.8 has a higher fibre fraction, so there could have been less matrix-fibre wetting [95]. Alternatively, the increased fibre content could be leading to increased stress concentration leading to more premature failure.

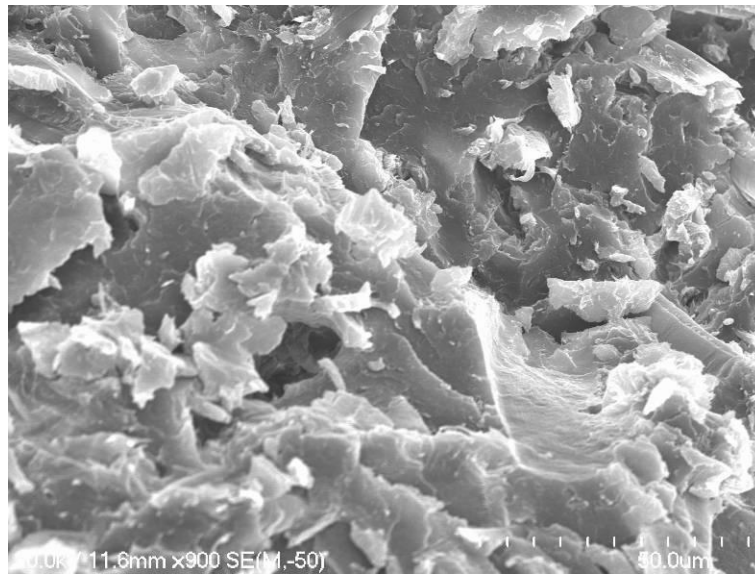


Figure 4.9 SEM of fracture surface of 30 wt% hemp/ PLA100°C 24hrs sample at 10mm/min

Figure 4.9 shows the fracture surface of a sample of PLA/30 wt % hemp annealed at 100°C for 24 hours, which differs vastly from the control sample (Figure 4.8) due to more visible fibre fracture and the lack of fibre pull-out.

SEM observations show that there is a distinct difference between unannealed and annealed samples' fracture surfaces. Elevated crystallinity and transcrystallinity on fibres are surmised to contribute to this difference in appearance.

4.2.2 Differential Scanning Calorimetry (DSC)

DSC heating thermographs for PLA, 15 wt% hemp/PLA and 30 wt% hemp/PLA are illustrated in Figures 4.10, 4.11 and 4.12 respectively. The thermographs were recorded for the range from 25°C up to 200°C. They each consist of seven plots representing a control sample (labelled 1) and 6 different annealing conditions used (labelled 2-7). The control and low temperature (70°C) annealed samples mostly demonstrate three successive transitions upon heating, namely: a glass transition stage (T_g) represented by a trough at around 50°C-60°C, exothermic cold-crystallisation (T_{CC}) represented by a peak at around 100°C-125°C and an endothermic melting stage (T_m) represented by a trough at around 150°C. Regarding samples that had been annealed at 100°C, there were no T_g or T_{CC} peaks, giving credence to the presumption that the composite structure composition in all fibre fractions already consisted of a high degree of matrix crystallinity. It is even more apparent in higher fibre fractions due to the fibres acting as a nucleating agent, causing increased crystallinity during annealing [97].

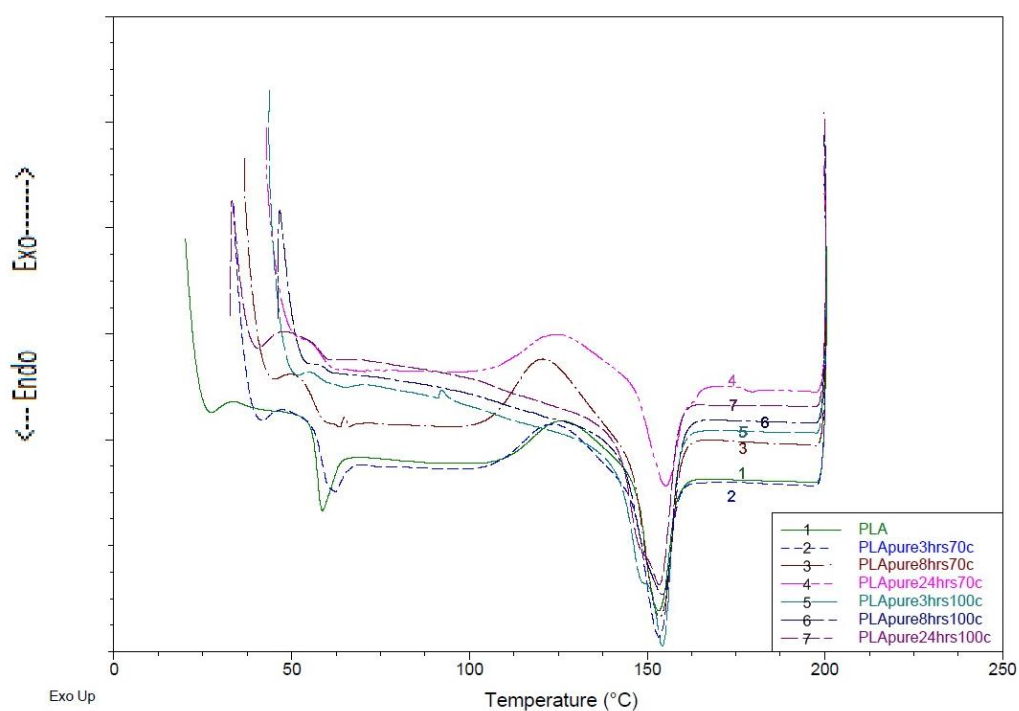


Figure 4.10 PLA DSC thermograph

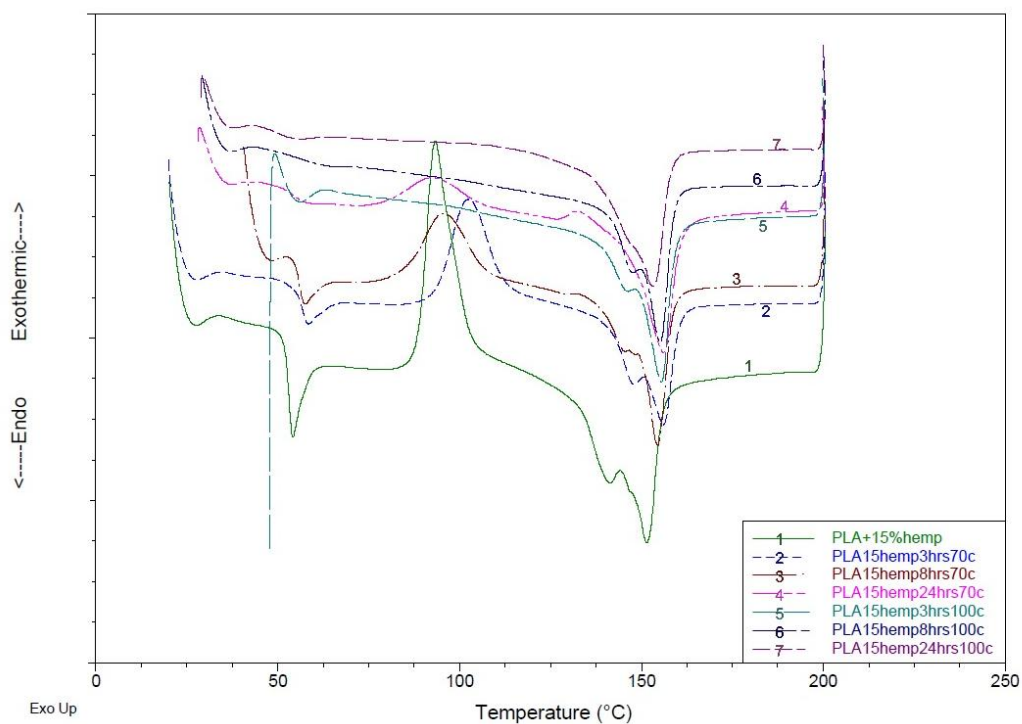


Figure 4.11 15 wt% hemp/PLA DSC thermograph

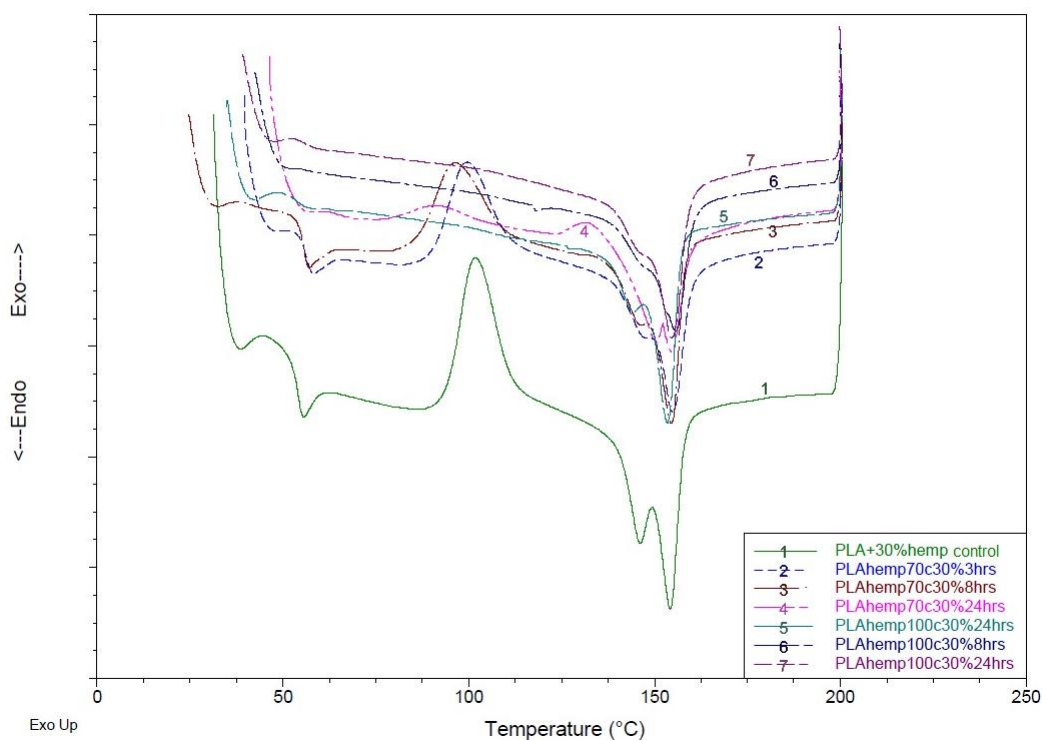


Figure 4.12 30 wt% hemp/PLA DSC thermograph

The exothermic cold crystallinity peak for the PLA control sample (Figure 4.10 plot 2) is at 126°C. Bigger cold crystallinity temperature peaks can be seen at a lower temperature ($\approx 100^\circ\text{C}$), for control samples of both 15 wt% hemp/PLA in

Figure 4.11 (plot 1) and 30 wt% hemp/PLA in Figure 4.12 (plot 1). This temperature reduction is attributed to the presence of fibre acting as a nucleating agent. For PLA (Figure 4.10 plots 5,6,7), 15 wt% hemp/PLA (Figure 4.11 plots 5,6,7) and 30 wt% hemp/PLA (Figure 4.12 plots 5,6,7) annealed at 100°C for 3, 8, and 24 hours, there are no cold crystallinity peaks or T_g troughs. This is likely to be due to higher amounts of crystallinity in the higher temperature annealed samples, leading to a stable and saturated structure where crystalline structures cannot form anymore. Annealing at around the cold crystallisation temperature (100°C) has made it possible for a highly crystalline structure to form than at lower temperatures.

Another point of interest is the presence of double melting peaks as observed in the DSC curves for all fibre fractions and at all annealing types (Figures 4.10, 4.11, 4.12 plots 1,2,3,4,5,6,7). These peaks can be attributed to the presence of crystallinity in the matrix structure and transcrystallinity encapsulating the fibre, which depends on the samples' thermal history, post manufacture as well as post annealing [98].

The percentage PLA crystallinity obtained using DSC data and analysis software are tabulated in Table 4.1 and graphed in Figure 4.13. The cold crystallisation temperatures for most hemp/PLA composites are lower than for PLA, as they already have a certain amount of crystallinity, due to the fibres' propensity to act as a nucleating interface [99]. These values and other comparisons can be observed in Table 4.1

Table 4.1 DSC data showing glass transition temperature (T_g), cold crystallisation temperature (T_{CC}), melting point temperature (T_m), enthalpy of melting (ΔH_m), cold crystallisation enthalpy (ΔH_{cc}) and crystallinity (X_{DSC})

Material Type	T_g (°C)	T_{CC} (°C)	T_m (°C)	ΔH_m (J/g)	ΔH_{cc} (J/g)	X_{DSC} (%)
PLA Control	58.69	126.80	153.20	11.97	8.89	3.31
PLA 70°C 3Hrs	62.30	123.16	153.31	15.68	8.80	7.40
PLA 70°C 8Hrs	65.09	120.76	153.57	19.46	15.02	4.77
PLA 70°C 24Hrs	N.A	125.48	155.23	10.85	9.78	1.15
PLA 100°C 3Hrs	N.A	N.A	154.18	45.22	N.A	47.55
PLA 100°C 8Hrs	N.A	N.A	154.13	40.64	N.A	42.62
PLA 100°C 24Hr	N.A	N.A	153.37	40.49	N.A	42.46
15wt% hemp/PLA control	54.20	93.31	151.42	38.68	34.14	5.74
15 wt% hemp/PLA 70°C 3Hrs	58.50	102.35	155.99	27.93	24.55	4.28
15 wt% hemp/PLA 70°C 8Hrs	57.61	95.57	154.44	32.00	17.29	18.61
15 wt% hemp/PLA 70°C 24Hrs	N.A	93.18	155.99	25.14	12.67	15.77
15 wt% hemp/PLA 100°C 3Hrs	N.A	N.A	155.45	53.94	N.A	66.97
15 wt% hemp/PLA 100°C 8Hrs	N.A	N.A	155.12	54.52	N.A	67.70
15 wt% hemp/PLA 100°C 24Hr	N.A	N.A	153.17	50.47	N.A	62.58
30 wt% hemp/PLA control	55.66	101.87	154.21	23.89	19.80	6.28
30 wt% hemp/PLA 70°C 3Hrs	51.60	99.47	154.87	19.78	14.44	8.20
30 wt% hemp/PLA 70°C 8Hrs	58.38	96.45	154.49	21.58	14.44	10.97
30 wt% hemp/PLA 70°C 24Hrs	N.A	91.45	154.48	23.45	N.A	34.49
30 wt% Hemp/PLA 100°C 3Hrs	N.A	N.A	153.48	47.26	N.A	71.06
30 wt% Hemp/PLA 100°C 8Hrs	N.A	N.A	155.63	43.96	N.A	65.99
30 wt% Hemp/PLA 100°C 24Hr	N.A	N.A	154.57	47.78	N.A	71.86

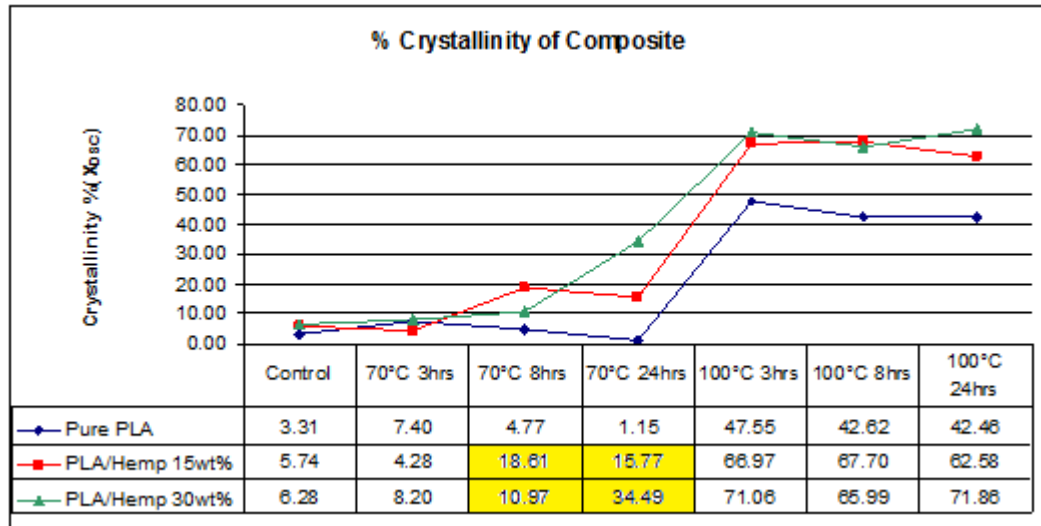


Figure 4.13 Percentage Crystallinity graph for control and treated samples of PLA and composites

The percentage crystallinity for the control PLA samples was around 3%. This increased slightly with the presence of fibre (see control for 15 wt% hemp /PLA and 30 wt% hemp /PLA). Only limited increase in crystallinity was observed for 3 hours at 70°C. On increased duration of annealing at 70°C, although PLA only sample were relatively unaffected, composites were seen to undergo a significant increase in crystallinity, supporting hemp acting as a nucleating agent. Further increases were seen as expected, as this is close to the cold crystallinity peak temperature for PLA (120°C)[100]. When annealing at 100°C was carried out giving crystallinity for PLA up to approximately 48% and up to 72% for composites.

4.2.3 X-Ray Diffraction Analysis (XRD)

XRD analysis was used to analyse the structure of PLA and hemp/PLA composites. In Figure 4.14, the PLA control sample did not have any significant peaks, which show that its crystallinity is very minute and indicates that it had poorly ordered PLA polymer chains [108]. The annealed PLA sample showed two

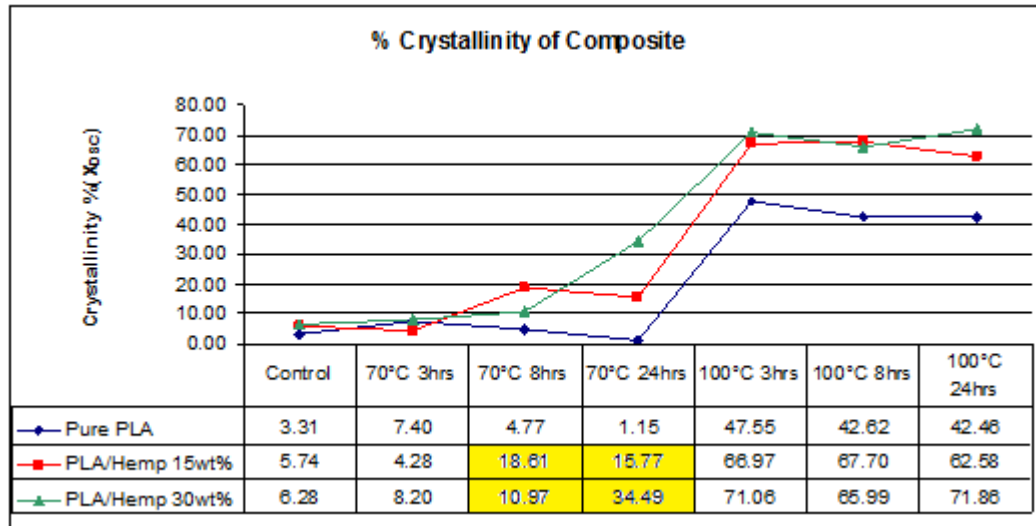


Figure 4.13 Percentage Crystallinity graph for control and treated samples of PLA and composites

The percentage crystallinity for the control PLA samples was around 3%. This increased slightly with the presence of fibre (see control for 15 wt% hemp /PLA and 30 wt% hemp /PLA in Figure 4.13). Only limited increase in crystallinity was observed for 3 hours at 70°C. On increased duration of annealing at 70°C, PLA only samples were relatively unaffected whereas composites were seen to undergo a significant increase in crystallinity (highlighted section in Figure 4.13), supporting that hemp fibres act as a nucleating agent. Further increases were seen as expected, when annealing at 100°C was carried out, as this is close to the cold crystallinity peak temperature for PLA (120°C)[100], where crystallinity reached up to approximately 48% for PLA and up to 72% for composites.

4.2.3 X-Ray Diffraction Analysis (XRD)

XRD analysis was used to analyse the structure of PLA and hemp/PLA composites. In Figure 4.14, the PLA control sample did not have any significant peaks, which show that its crystallinity is very minute and indicates that it had poorly ordered PLA polymer chains [108]. The annealed PLA sample showed two

peaks at $16^\circ \leq 2\theta \leq 17$ (020 crystallographic plane diffraction) and $18.5^\circ \leq 2\theta \leq 19.5$ (023 crystallographic plane diffraction) supporting the presence of crystallinity in the PLA matrix [98]. There are generally three distinct peaks visible for hemp/PLA fibre composites and their annealed samples at around $16^\circ \leq 2\theta \leq 17$, $18.5^\circ \leq 2\theta \leq 19.5$ and $22^\circ \leq 2\theta \leq 23$. From literature, it is known that the peak at $22^\circ \leq 2\theta \leq 23$ is influenced by the presence of hemp fibres because the peak at $22^\circ \leq 2\theta \leq 23$ represents the characteristic peak of cellulose I, in hemp fibre, which corresponds to the 002 crystallographic plane [109]. However, close to that peak, in the 121 crystallographic plane diffraction at $2\theta = 22.3^\circ$, there is also a very small PLA matrix contribution to the diffraction [98].

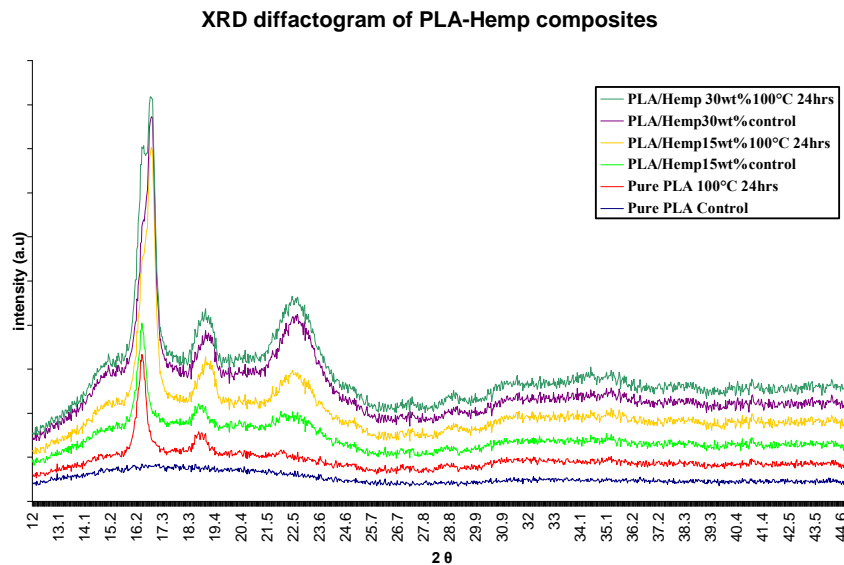


Figure 4.14 XRD diffractogram of Hemp/PLA composites

The crystallinity of the fibre in the control samples of 15 wt% hemp/PLA composite and 30 wt% hemp/PLA composite was found to be 59.2% and 52.9% respectively as shown in Table 4.2. These values are much less than those observed by other researchers when testing hemp fibres only [110, 111, 112]. It can be surmised that this reduction in fibre crystallinity is due to the extruding process, and its associated high temperatures (180°C) and shear forces resulting in

grinding of the fibres. From that, there is a possibility that the hemp fibres could have undergone thermal as well as mechanical degradation while being compounded with the PLA matrix. However, the cellulose crystallinity in the annealed samples of hemp/PLA composite are even less, being 44.3%, compared to 59.2% for 15 wt % hemp/PLA control sample and 37.7%, compared to 52.9% for 30 wt % hemp/PLA control sample. This low crystallinity when compared to hemp fibre only and compounded hemp fibres in composites can be due to degradation and further moisture loss in the hemp component of the composite specimen. These values cannot be taken to be absolute though, due to the effect of the presence of possible PLA matrix crystallinity that affects them.

Table 4.2 Crystallinity I values for cellulose components of hemp/PLA composite.

Hemp/PLA Composite variant	15 wt% hemp/PLA control	15wt% hemp/PLA 100°C 24Hrs	30wt% hemp/PLA control	30wt% hemp/PLA 100°C 24Hrs
Crystallinity (%)	59.2	44.3	52.9	37.7

4.2.4 Polarised Optical Microscope (POM) analysis

Polarised optical microscopy was used to observe single fibre with PLA pressed between cover slips as well as composite fracture toughness sample crack profiles. Figure 4.15 shows fibres embedded in PLA between two glass slips demonstrating differences in crystallinity due to different fibre treatments. Large differences in colour contrast occurred with small differences in PLA film thicknesses and optical focusing and filtering, however, regarding structure, the micrographs are representative of all samples seen.

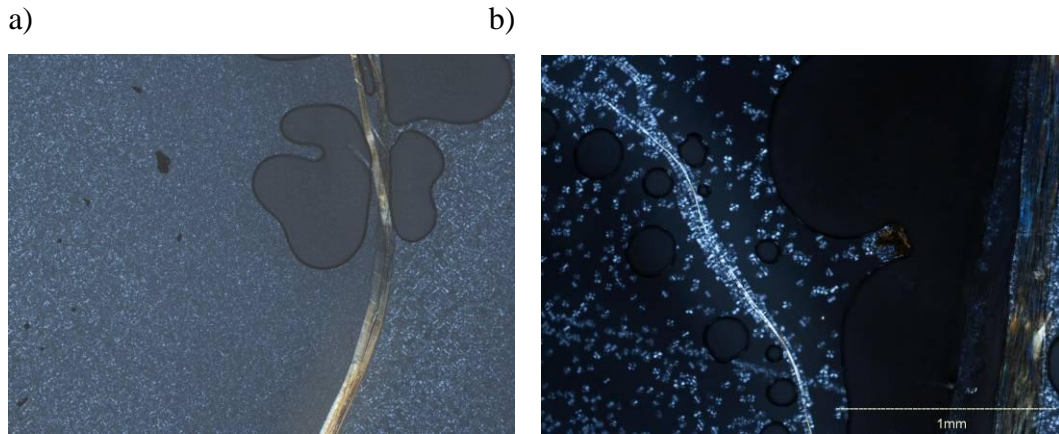


Figure 4.15 fibres embedded in PLA between two glass slips(200x magnification): a): Untreated fibre in PLA b): Treated fibre in PLA

In Figure 4.15b, it can be seen that the treatment of hemp fibres with alkali solution has resulted in the appearance of spherulites within the matrix bulk and transcrystallinity occurring on the fibre surfaces supporting their function as a nucleating surface [101]. Figure 4.15a demonstrates the total absence of transcrystallinity on the untreated fibre surface.

Crack profiles of tested fracture toughness sample were compared for samples of different fibre loadings from the control batch and for the batch that had been annealed at 100°C for 24 hours, as they showed the greatest visual variance.

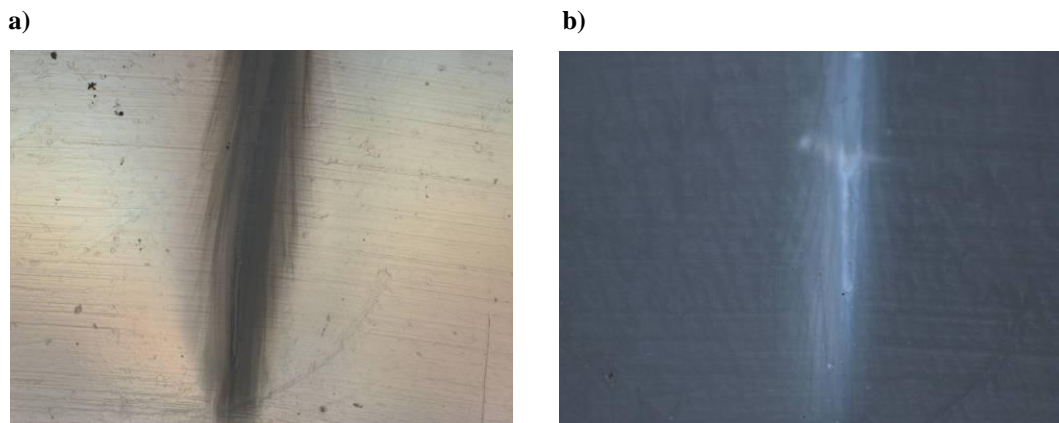
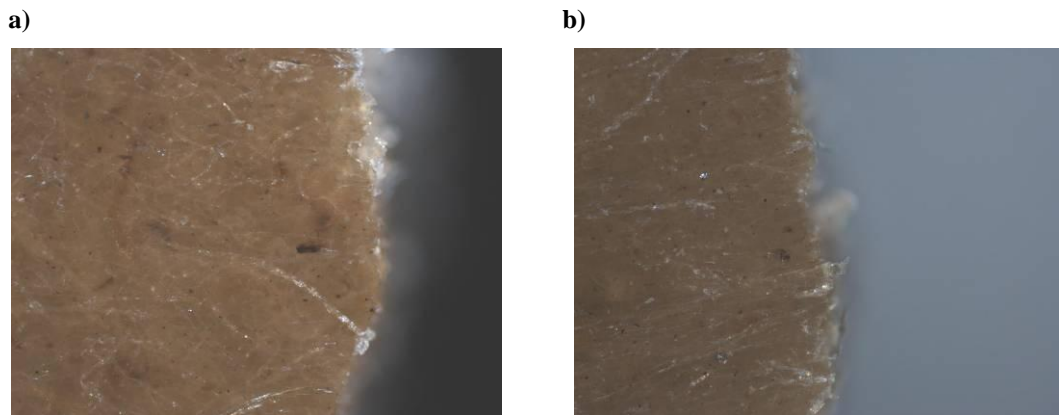


Figure 4.16 Fracture toughness samples showing crack profiles for a) PLA control b) PLA annealed 100°C 24hrs

Figures 4.15 show the fracture toughness test samples crack profiles for PLA control and PLA annealed at 100°C for 24 hours. In Figure 4.16a, the craze formation path along the crack tip region for the PLA samples show that it utilises a larger volume and is more spread out as generally observed in an amorphous polymer [102] as opposed to PLA annealed at 100°C in Figure 4.16b where the crack path is more confined. This is attributed to an increase in crystallinity in the annealed sample; the cracks are assumed to propagate directed to some extent by crystallinity, although whether this is within crystallinity or at the amorphous/crystalline PLA interface is unknown.



**Figure 4.17 Fracture toughness samples showing crack profiles for, a)- 15 wt% hemp/PLA
b)- 15 wt% hemp/PLA 100°C 24 hours**

The crack propagation paths appear to be similar for the composites with different annealing durations as seen in Figures 4.17 a and 4.17 b, suggesting any variation in crack propagation is visually disguised by the presence of fibres in the matrix. There is, however a slight translucence that can be discerned in the control sample in Figure 4.17a when compared to the annealed sample in Figure 4.17b. The crack propagation path is also obscured due to the addition of fibres where it induces the direction and path of crack propagation to follow the weakest fibres possible.

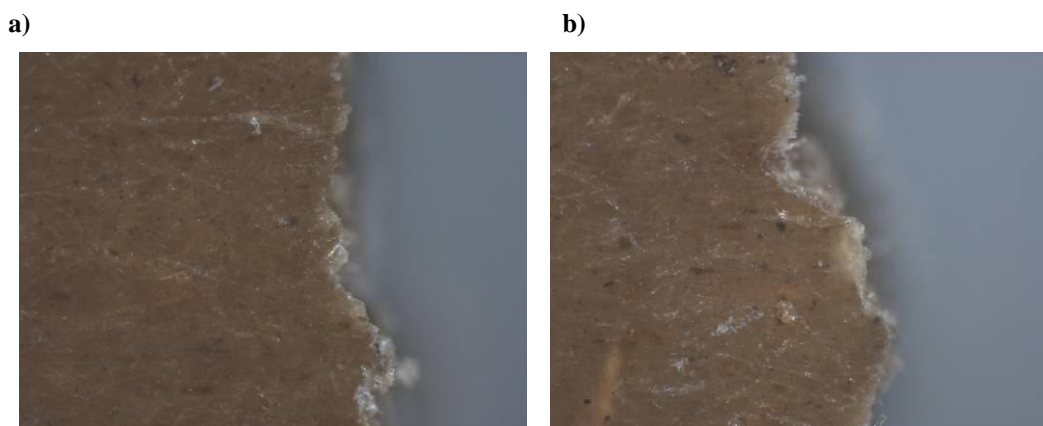
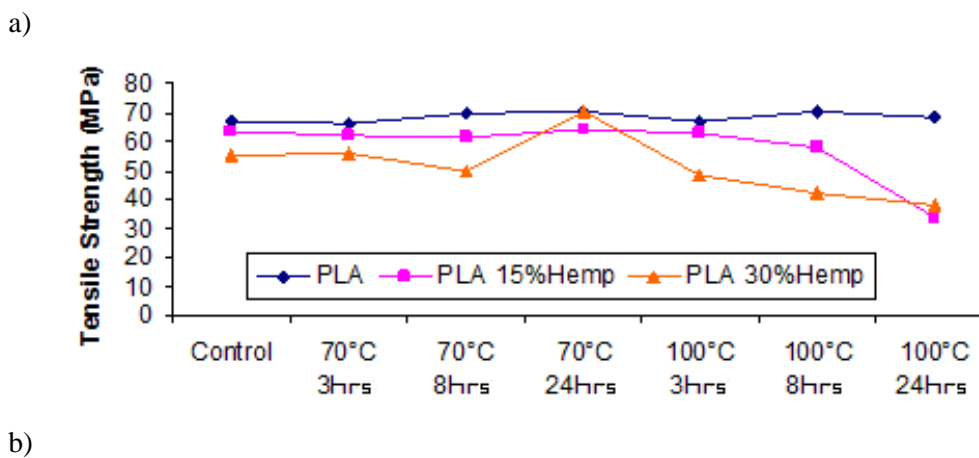


Figure 4.18 Fracture toughness samples showing crack profiles for a)- 30 wt% hemp/PLA,
b)- 30 wt% hemp/PLA 100°C 24 hours

The addition of 30 wt % of hemp fibre has resulted in the saturation of the PLA matrix resulting in transcrystallinity on the fibre surface. This transcrystallinity has resulted in the irregular crack profiles, when opposed to 15 wt% hemp/PLA composites. Again, the crack propagation paths appear to be similar for composites with different annealing schedules when Figure 4.18 a and 4.18 b is compared, which makes the assumption that any visual differences in crack propagation are masked by the incidence of fibres in the matrix material.

4.2.5 Tensile Strength and Fracture Toughness (K_{1C})



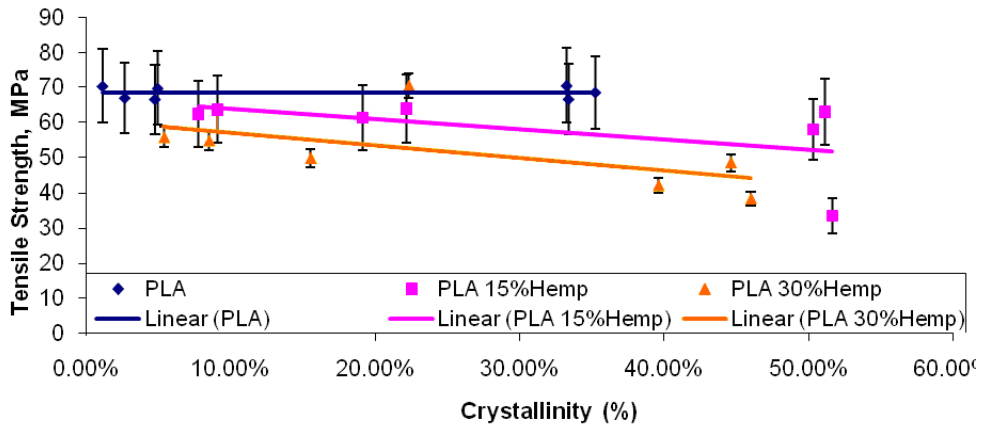
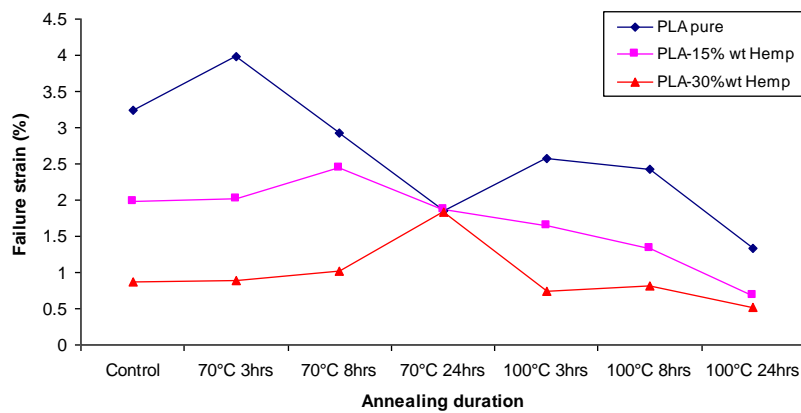


Figure 4.19: a) Tensile strength for hemp/PLA composites at 10mm/min b) Tensile strength vs. crystallinity for hemp/PLA composites

Tensile strength of PLA and composite samples of various fibre weight percentages was tested and Figure 4.19a displays the results of tensile strength versus annealing schedule, translated in Figure 4.19b relative to crystallinity. The tensile strength (Figure 4.19a) for PLA was found to be generally unaffected by annealing level and the associated change in crystallinity (Figure 4.19b). However, there appears to be a small general reduction in tensile strength for the hemp/PLA composites (15 and 30 wt %), as crystallinity increases as seen in Figure 4.19b [106].

a)



b)

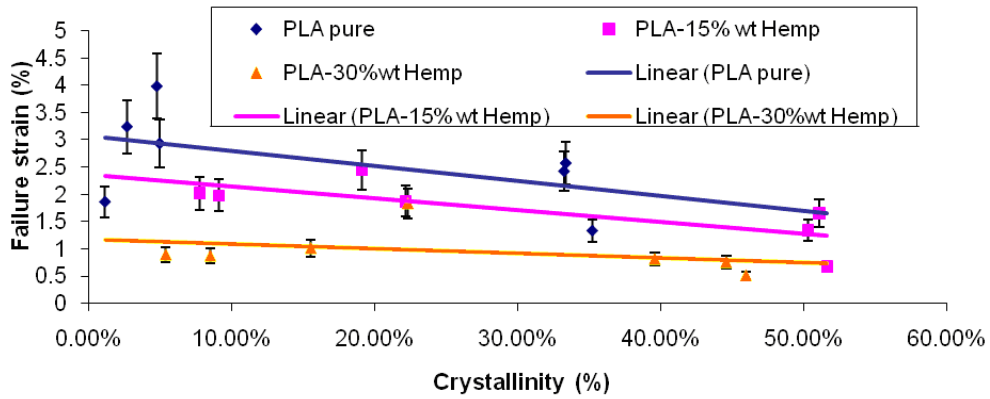
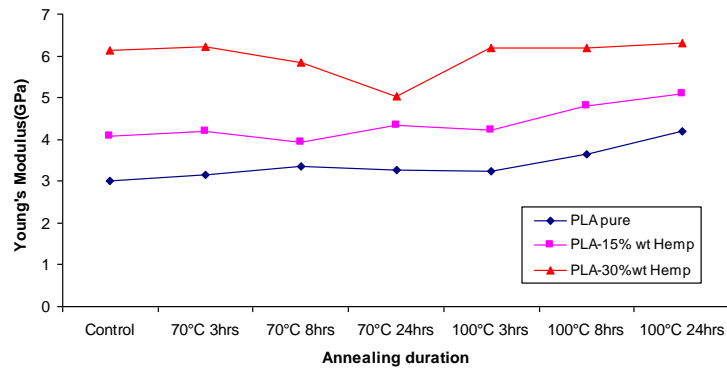


Figure 4.20: a) Failure strain (%) for hemp/PLA composites at 10mm/min, b) Failure strain (%) vs. crystallinity (%) for hemp/PLA composites

Failure strain for the PLA and composite samples (Figure 4.20) shows a general trend of decline with increasing of crystallinity. It would appear that crystallinity has resulted in the matrix material less able to deform plastically, increasing its propensity for brittle failure, for all fibre fractions.

a)



b)

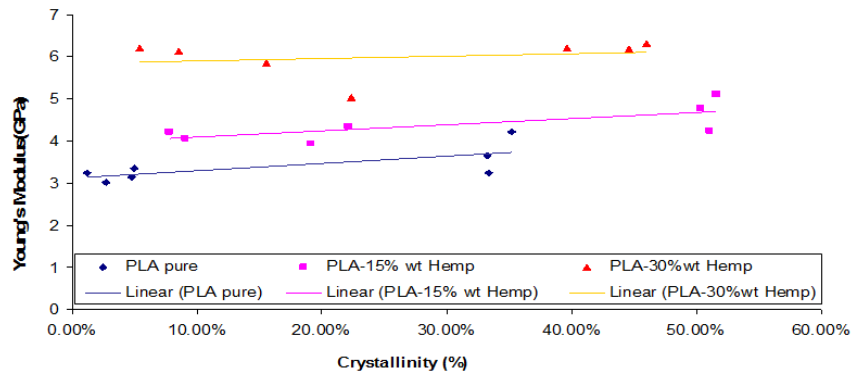
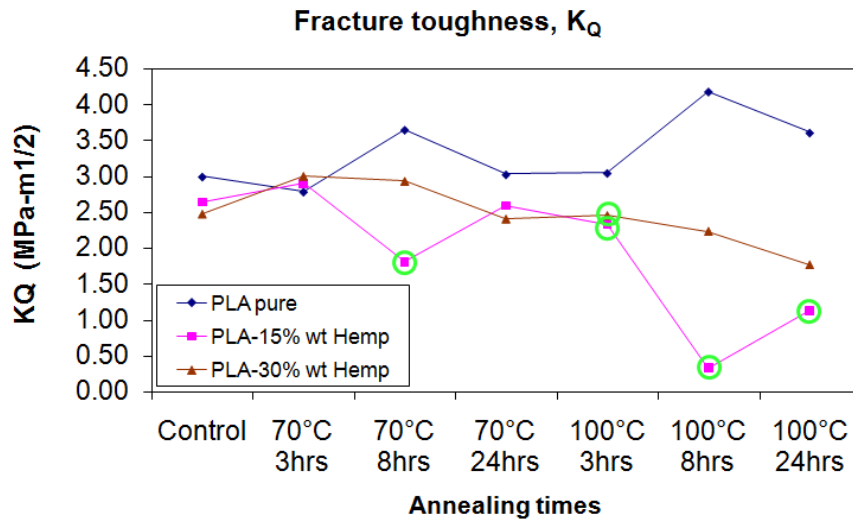


Figure 4.21: a) Young's modulus values for hemp/PLA composites at 10mm/min, b) Young's modulus vs. crystallinity (%) for hemp/PLA composites

Figure 4.21 depicts the Young's modulus values for PLA and composites with 15 and 30 wt% hemp. It suggests a slight increase in Young's modulus with increased crystallinity for PLA and composites.

a)



b)

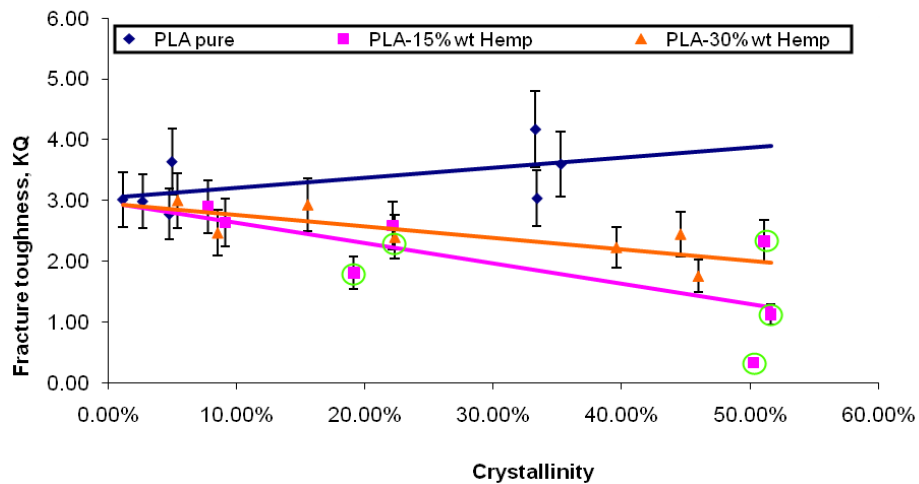
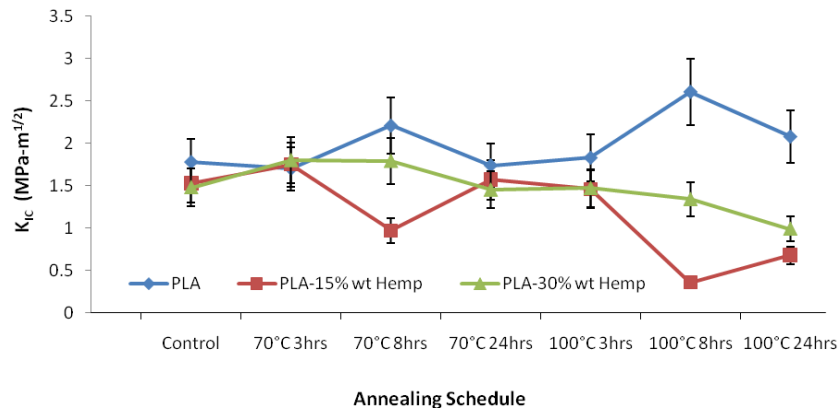


Figure 4.22: a) Fracture toughness for hemp/PLA composites at 10mm/min, b) Fracture toughness vs. crystallinity for hemp/PLA composites

Figure 4.22 shows results from fracture toughness testing, showing the fracture toughness values, K_Q relative to annealing duration. Out of all the K_Q values, it was found that only 5 test specimen sets had met the criterion for critical-stress-intensity factor, K_{IC} . They are: 15 wt% hemp/ PLA annealed at 70°C for 8 hours, 100°C for 3 hours, 100°C for 8 hours, and 100°C for 24 hours; and 30 wt% hemp/

Figure 4.21 depicts the Young's modulus values for PLA and composites with 15 and 30 wt% hemp. It suggests a slight increase in Young's modulus with increased crystallinity for PLA and composites.

a)



b)

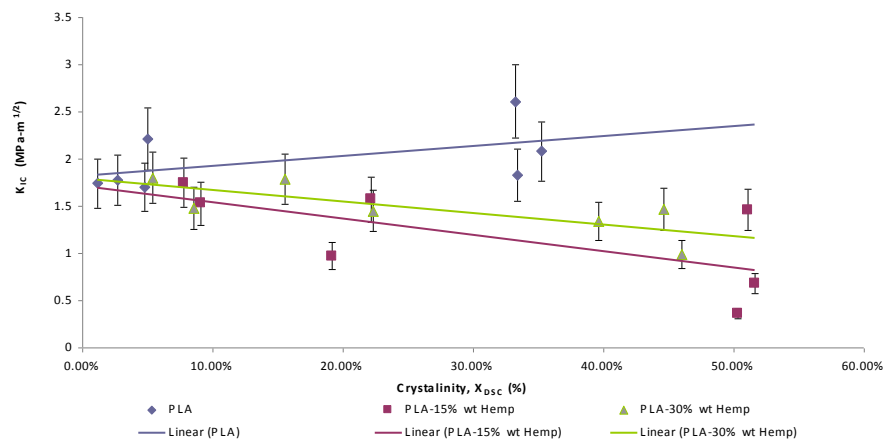


Figure 4.22: a) Fracture toughness for hemp/PLA composites at 10mm/min, b) Fracture toughness vs. crystallinity for hemp/PLA composites

Figure 4.22 shows results from fracture toughness testing, showing the critical stress intensity factor, K_{IC} , relative to annealing duration and crystallinity. The decrease in K_{IC} values for composites generally supports that fracture toughness decreases with the increase of crystallinity, due to the increased ease with which cracks propagate through the structure via crystallinity encouraged by stress concentration as an effect of fibre loading [107].

PLA annealed at 70°C for 24 hours, circled in green in Figure 4.30a and b. Although the conditions $2B < W < 4B$ were met. It seems that higher loading speeds or larger sample dimensions would be required for to reach K_{IC} . The decrease in K_Q values for composites for composite generally supports that fracture toughness decreases with the increase of crystallinity which is likely due to the increased ease with which cracks propagate through the structure via crystallinity encouraged by stress concentration due to fibres [107].

4.2.6 Dynamic Mechanical Thermal Analysis (DMTA)

The effect of increased crystallinity on the storage modulus (E'), Loss modulus (E'') and damping factor ($\tan \delta$) at two different frequencies (1Hz and 10 Hz) for hemp/PLA fibre composites of two fibre loadings (15 wt% and 30 wt%) and at two stages of annealing (annealed and unannealed), is demonstrated in Figures 4.23, 4.24, 4.25, 4.26, 4.27 and 4.28. The experiment was run for temperature ramp range from room temperature up to 130°C at a rate of 5°C/min.

Comparing Figures 4.23 and 4.24, higher E' and E'' are retained at higher experimental ramp temperatures for the PLA annealed sample (Figure 4.24) compared to the control sample. $\tan \delta$, is also lower, suggesting that the mobility of the material has decreased significantly at higher temperatures, being more rigid when compared to the PLA control sample (Figure 4.23). These more rigid features can be attributed to an increase of crystallinity and the associated increase in secondary bonds which would make the material less fluid and more stable at high temperatures, making PLA more heat resistant at higher temperatures, mainly due to the existence of crystallinity, as seen by Park et al.[103] and Pluta et al[98].

4.2.6 Dynamic Mechanical Thermal Analysis (DMTA)

The effect of increased crystallinity on the storage modulus (E'), Loss modulus (E'') and damping factor ($\tan \delta$) at two different frequencies (1Hz and 10 Hz) for hemp/PLA fibre composites of two fibre loadings (15 wt% and 30 wt%) and at two stages of annealing (annealed and unannealed), is demonstrated in Figures 4.23, 4.24, 4.25, 4.26, 4.27 and 4.28. The experiment was run for temperature ramp range from room temperature up to 130°C.

Comparing Figures 4.23 and 4.24, higher E' and E'' are retained at higher temperatures for the PLA annealed sample (Figure 4.24), when compared to the control sample (Figure 4.23). $\tan \delta$, is also lower, suggesting that the mobility of the material has decreased significantly at higher temperatures, being more rigid when compared to the PLA control sample (Figure 4.23). These more rigid features can be attributed to an increase of crystallinity and the associated increase in secondary bonds which would make the material less fluid and more stable at high temperatures, making PLA more heat resistant at higher temperatures, mainly due to the existence of crystallinity, as seen by Park et al.[103] and Pluta et al[98].

The peaks of $\tan \delta$ occur at the glass transition temperature range (T_g) of PLA material; the peak of which in Figure 4.24 is smaller than in Figure 4.23. The E'' in Figure 4.24 follows a similar trend, peaking at T_g , and does not lose rigidity as obviously as observed in Figure 4.23, where it starts to waver beyond 100°C . This wavering is seen for the three material properties in Figure 4.23 but not for Figure 4.24. This is due to the presence of crystallinity ($X_C = 42.46\%$) in annealed PLA (Figure 4.24), preventing polymer softening, leading to more material rigidity and less loss of elasticity at higher operating temperatures.

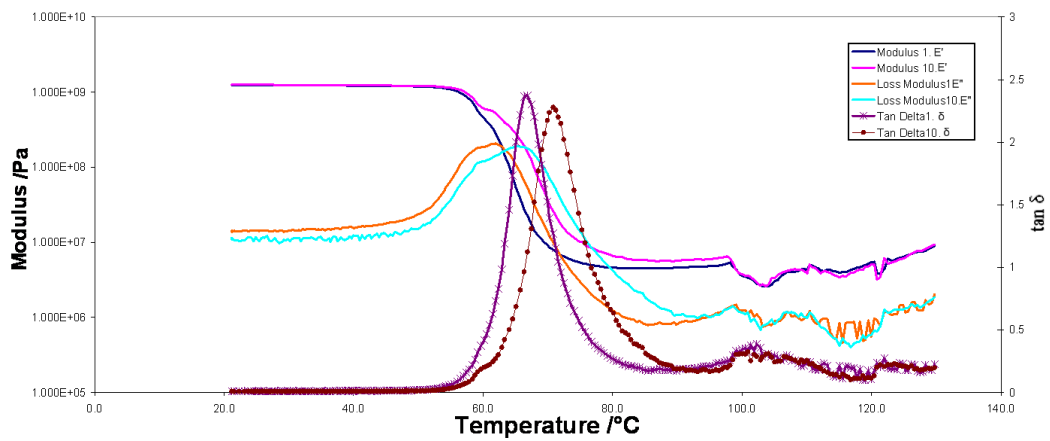


Figure 4.23 E' , E'' and $\tan \delta$ for PLA control at 1Hz and 10Hz

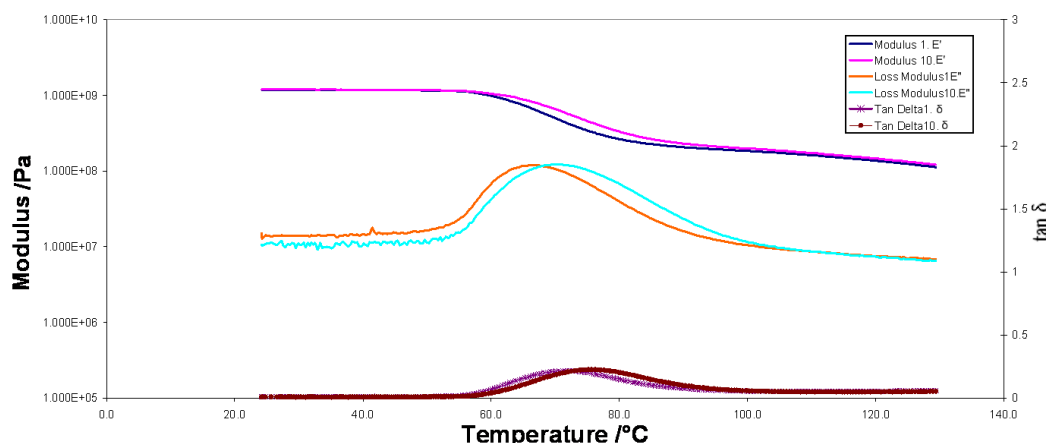


Figure 4.24 E' , E'' and $\tan \delta$ for PLA 100°C 24Hrs at 1Hz and 10Hz

In the case of the composite control specimens in Figures 4.25 and 4.27 the $\tan \delta$ peaks were much smaller than for the PLA control, as well as E' and E''

curves, as the specimens' mobility were restricted by the presence of fibres interfacing with the matrix. The effect of fibre loading was a small one, with more fibre (30 wt% Figure 4.27) seen to result in a smaller $\tan \delta$ peak when compared to less fibre (15 wt% Figure 4.25) The combination of fibre and transcrystallinity seems to have obstructed the mobility of the composite at elevated temperatures, increasing its rigidity. Even so, the wavering of material properties still occurred slightly (as was seen in Figure 4.23 for PLA only control sample), albeit at a lower temperature, at around 80°C in Figures 4.25 and 4.27. The $\tan \delta$ peaks for T_g range peaks for composite control specimens in Figures 4.25 and 4.27 did not change much as the operating ramp temperature increased, compared to the PLA control sample [105].

The E' , E'' and $\tan \delta$ in Figures 4.26 and 4.28 also acted in a similar manner to that in Figure 4.24, suggesting that damping has been reduced by the matrix crystallinity in addition to transcrystallinity on the fibres and fibre-matrix interface in the composite. The effect of fibre loading is less apparent at these high crystallinities.

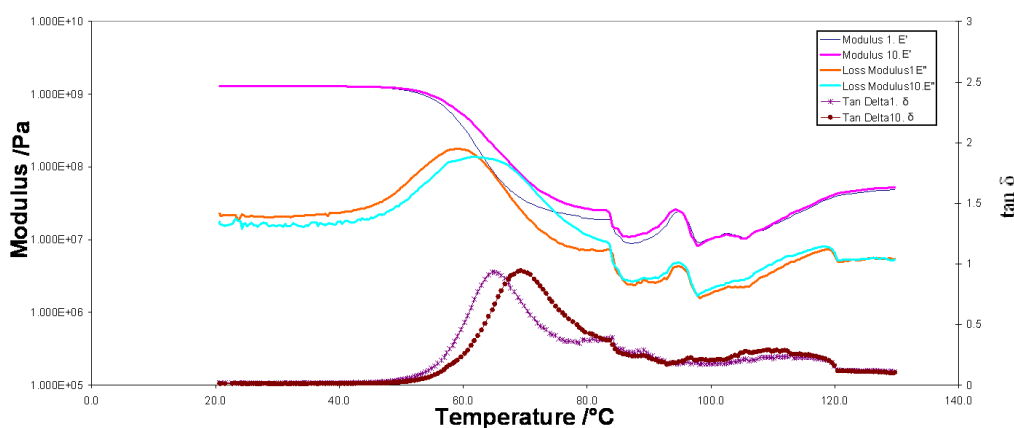


Figure 4.25 E' , E'' and $\tan \delta$ for 15 wt % hemp/PLA control at 1Hz and 10Hz

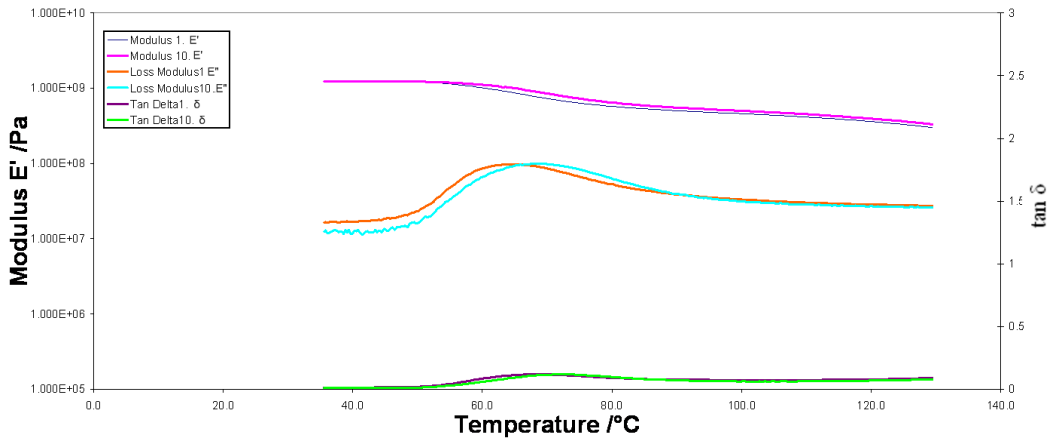


Figure 4.26 E', E'' and tan δ for 15 wt % hemp/PLA 100°C 24Hrs at 1Hz and 10Hz

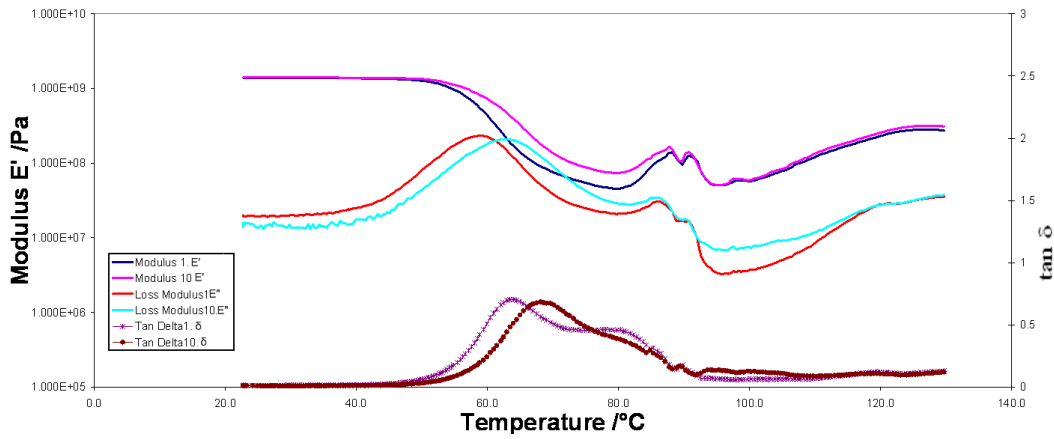


Figure 4.27 E', E'' and tan δ for 30 wt % hemp/PLA Control at 1Hz and 10Hz

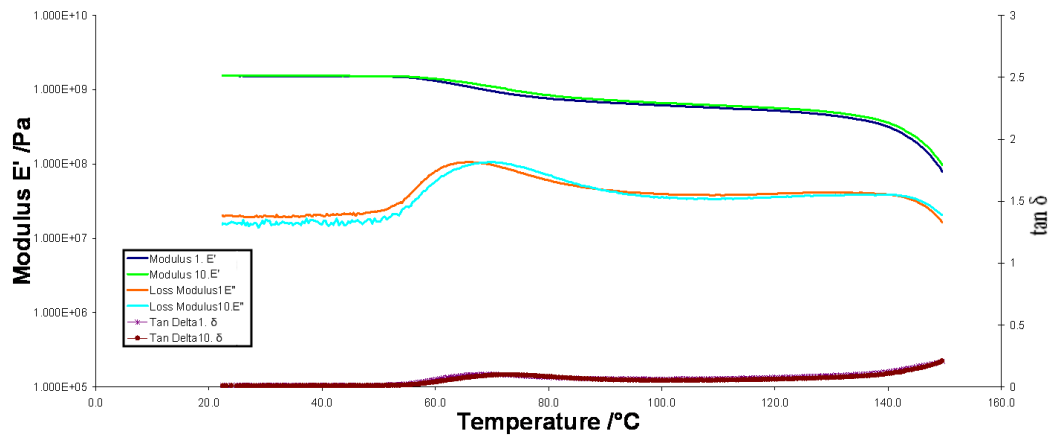


Figure 4.28 E', E'' and tan δ for 4.27 30 wt % hemp/PLA 100°C 24Hrs at 1Hz and 10Hz

Chapter 5: Conclusions and Recommendations for Future Work

5.1 Conclusions

To summarise, PLA pellets were compounded with alkali treated hemp fibres and moulded to create reinforced composite samples at two different fibre fractions 15 wt% and 30 wt% and were annealed at 70°C and 100°C for 3 hours, 8 hours and 24 hours and compared to PLA samples. The specimens were subsequently analysed for their tensile strength, fracture toughness and crystallinity. The crystallinity of the specimens were also tested using differential scanning calorimetry (DSC) and X-ray diffraction (XRD) and it was found that there was an increase in crystallinity with variations of annealing schedules. It was found that tensile strength and Young's modulus decreased slightly with variation in crystallinity leading from variation in annealing schedules for all PLA and PLA composites of all fibre fractions. Fracture toughness for PLA samples increases slightly with increasing crystallinity whereas 15 wt% and 30 wt% hemp composites demonstrated reducing fracture toughness with increasing levels of crystallinity. DMTA analysis shows the material stability of the annealed samples at higher temperatures, where its stiffness is maintained.

Crystallinity in hemp/PLA composites can be induced via annealing and produces unique results on various material properties and results in a physically stable material at higher temperatures.

5.2 Recommendations for future work

It is surmised that more research needs to be done to explore controlling crystallinity in the manufacture of hemp and PLA composites. Areas of interest to be examined include:-

- quenching molten samples using liquid nitrogen
- controlled quenching during manufacture
- single step compounding and injection moulding
- carry out dual cantilever, compression testing, low temperature (below 0°C) test runs using DMTA
- increased and varying loading rates beyond 10mm/min for fracture toughness testing
- samples could be taken from different sections of the specimen to ensure even distribution of fibre throughout the sample when DSC and XRD analysis is carried out,
- Also, thicker test specimens could be used when doing fracture toughness tests in order to prevent noncompliance with critical-stress intensity factor (K_{IC}), criteria.

References

- [1] Klaus Friedrich, Stoyko Fakiro Zhong Zhang, Polymer composites: from nano-to-macro-scale, Springer, (2005)
- [2] Daniel Gay, Suong V. Hoa, Stephen W. Tsai, Composite Materials Design and Applications, CRC press (2003)
- [3] Y. Chen, O. Chiparus, L. Sun, I. Negulescu, D. V. Parikh and T. A. Calamar, Natural Fibers for Automotive Nonwoven Composites, Journal of Industrial Textiles (2005) 35-47
- [4] Muhammad Pervaiz, Mohini M.Sain, Carbon storage potential in natural fiber composites, Resources, Conservation and Recycling 39 (2003) 325-340
- [5] Paul Wambua, Jan Ivens, Ignaas Verpoest, Natural fibres: can they replace glass in fibre reinforced plastics?, Composites Science and Technology 63 (2003) 1259–1264
- [6] M.H.Hartmann, Biopolymers from Renewable Resources, Springer-Verlag ,Berlin, (1998) pp.367–411.
- [7] Maya Jacob John, Sabu Thomas, Biofibres and biocomposites, Carbohydrate Polymers 71 (2008) 343–364
- [8] V.R. Gowariker, N. V. Viswanathan, Jayadev Sreedhar, Polymer Science New Age International (P) Ltd (1986)
- [9] J.A. Brydson, Plastic Materials (Seventh Edition) Butterworth-Heinemann, (1999)
- [10] Angela M.Harris, Ellen C.Lee, Improving Mechanical Performance of Injection Molded PLA by Controlling Crystallinity, Journal of Applied Polymer Science, Vol.107, (2008) 2246–2255
- [11] D. N. Saheb, and J. P. Jog, Natural fiber polymer composites: A review, Advances in Polymer Technology 18 (1999) 351 - 363
- [12] J. H. Song, R. J. Murphy, R. Narayan and G. B. H. Davies, Biodegradable and compostable alternatives to conventional plastics, Phil. Trans. R. Soc. B, 364 (2009) 2127-2139
- [13] Anne-Marie M. Baker Joey Mead, Charles A. Harper, Handbook of Plastics, Elastomers, and Composites, McGraw-Hill

- [14] K. Oksman, M. Skrifvars, and J. F. Selin, Natural fibres as reinforcement in polylactic acid (PLA) composites, *Composites Science and Technology* 63 (2003) 1317-1324.
- [15] S.V.Joshi, L.T.Drzal, A.K.Mohanty, S.Arora, Are natural fiber composites environmentally superior to glass fiber reinforced composites? *Composites: Part A* 35 (2004) 371–376
- [16] Md. Mominul Haque, Mahbub Hasan, Md.Saiful Islam, Md. Ershad Ali, Physico-mechanical properties of chemically treated palm and coir fiber reinforced polypropylene composites, *Bioresource Technology* 100 (2009) 4903
- [17] M. Garcia, I. Garmendia, and J. Garcia, Influence of natural fiber type in eco-composites, *Journal of Applied Polymer Science* 107 (2008) 2994.
- [18] M. S. Huda, L. T. Drzal, M. Misra, A. K. Mohanty, K. Williams, and D. F. Mielewski, A study on biocomposites from recycled newspaper fiber and poly(lactic acid), *Industrial and Engineering Chemistry Research* 44 (2005) 5593
- [19] L.Davies, J.W. Cherrie, Airborne fibre concentrations in a glass continuous filament factory, *Annals of Occupational Hygiene* 36:6 (1992) 609-627
- [20] P.Mutje, A.Lopez, M.E.Vallejos, J.P.Lopez, F.Vilaseca, Full exploitation of Cannabis sativa as reinforcement/filler of thermoplastic composite materials, *Composites: Part A* 38 (2007) 369–377
- [21] Mirjana Kostic, Biljana Pejic, Petar Skundric, Quality of chemically modified hemp fibers, *Bioresource Technology* 99 (2008) 94–99
- [22] Sail-cloth: A global fabric, *Tinctoria* Vol 102: 5 (2005)
- [23] K.L.Pickering, G.W.Beckermann, S.N.Alam, N.J.Foreman Optimising industrial hemp fibre for composites, *Composites: Part A* 38 (2007) 461–468
- [24] Muhammad Pervaiz, Mohini M.Sain, Carbon storage potential in natural fiber composites, *Resources, Conservation and Recycling* 39 (2003) 325-340
- [25] Mechtler, Klemens, Bailer, Josef, De Hueber, Karl, Variations of Δ^9 -THC content in single plants of hemp varieties, *Industrial Crops and Products*, vol 19, no. 1, (2004) 19-24
- [26] AFP/ Getty Images and Luke Zigovits
- [26] Hernandez, A, Westerhuis, W, van Dam, J.E.G., Microscopic study on hemp bast fibre formation, *Journal of Natural Fibers* 3 -4 (2005) 1-12

- [27] Bei Wang, Sain, M., Oksman, K, Study of structural morphology of hemp fiber from the micro to the nanoscale. *Applied Composite Materials*, v 14, n 2, (2007) 89-103
- [29] Ouajai, S. and Shanks, R.A., Composition, structure and thermal degradation of hemp cellulose after chemical treatments. *Polymer Degradation and Stability*, 89(2), (2005). 327-335.
- [30] [31] Rowell, R.M., Han, J.S., and Rowell, J.S., Characterization and factors effecting fiber properties, in *Natural Polymers and Agrofibrils Composites*, E.L.A.L.a.M. Froline, L.H.C., Editor. 2000, Embrapa Instrumentacao Agropecuaria: Sao Carlos, Brazil. p. 115-134
- [32] Walker, J.C.F., Basic wood chemistry and cell wall ultrastructure, in *Primary Wood Processing*. 1993, Chapman and Hall: London. p. 23-67.
- [33] R.M.Rowell. A new generation of composite materials from agro-based fibre. *The Third International Conference on Frontiers of Polymers and Advanced Materials*. 1995. Kuala Lumpur, Malaysia
- [34] Eichhorn, S.J., Baillie, C.A., Zafeiropoulos, N., Mwaikambo, L.Y., Ansell, M.P., Dufresne, A., Entwistle, K.M., Herrera-Franco, P.J., Escamilla, G.C., Groom, L., Hughes, M., Hill, C., Rials, T.G., and Wild, P.M., Current international research into cellulosic fibres and composites. *Journal of Materials Science*, 2001. 36(9): p. 2107-2131
- [35] Shin, Soo-Jeong, Sung, Yong Joo, Improving enzymatic hydrolysis of industrial hemp (*Cannabis sativa* L.) by electron beam irradiation, *Radiation Physics and Chemistry*, vol 77, no 9 (2008) 1034-1038
- [36] Y. Chen, O. Chiparus, L. Sun, I. Negulescu, D. V. Parikh and T. A. Calamar, Natural Fibers for Automotive Nonwoven Composites, *Journal of Industrial Textiles* (2005) 35-47
- [37] Wibowo,A.C., Mohanty,A.K., Misra,M., and Drzal,L.T., Injection molded eco-friendly biocomposites from natural fiber and cellulosic bio-plastic *Technical Paper - Society of Manufacturing Engineers*, p 79-84, 2004, ICCM-14
- [38] J.A. Brydson, *Plastic Materials (Seventh Edition)* Butterworth-Heinemann, (1999)
- [39] Byrom, D.*Biomaterials*, D. Byrom, Ed., Stockton Press, New York, (1991)

- [40] G.S. Brady, H.R. Clauser, J.A. Vaccari, *Materials Handbook* (15th edition), McGraw Hill
- [41] [42] [44] Erwin T.H.Vinka, Karl R. Rabagob, David A. Glassnerb ,Patrick R .Gruberb, Applications of lifecycle assessment to NatureWorks™ polylactide (PLA)production
- [43] Donald Garlotta, A Literature Review of Poly(Lactic Acid), *Journal of Polymers and the Environment*, Vol.9, No.2, (2002)
- [45] D. N. Saheb, and J. P. Jog, Natural fiber polymer composites: A review, *Advances in Polymer Technology* 18 (1999) 351 - 363
- [46] Wang, H.M., Postle, R., Kessler, R.W., and Kessler, W., Removing pectin and lignin during chemical processing of hemp for textile applications. *Textile Research Journal*, 73(8): (2003) 664-669.
- [47] [48] M. Abdelmouleh, S. Boufi, M. N. Belgacem, and A. Dufresne, Short natural-fibre reinforced polyethylene and natural rubber composites: Effect of silane coupling agents and fibres loading, *Composites Science and Technology* 67 (2007) 1627.
- [49] J. H. Song, R. J. Murphy, R. Narayan and G. B. H. Davies, Biodegradable and compostable alternatives to conventional plastics, *Phil. Trans. R. Soc. B*, 364 (2009) 2127-2139
- [50] Hanwen Xiao, Wei Lu, Jen-Taut Yeh, Effect of Plasticizer on the Crystallization Behavior of Poly(lactic acid) *Journal of Applied Polymer Science*, Vol.113, (2009) 112–121
- [51] Zhongjie Ren, Lisong Dong, Yuming Yang, Dynamic Mechanical and Thermal Properties of Plasticized Poly(lactic acid) *Journal of Applied Polymer Science*, Vol.101, (2006) 1583–1590
- [52] R. Masirek, Z. Kulinski, D. Chionna, E. Piorkowska, and M. Pracella, Composites of poly(L-lactide) with hemp fibers: Morphology and thermal and mechanical properties, *Journal of Applied Polymer Science* 105 (2007) 255.
- [53] Yeng-Fong Shih, Chien-Chung Huang and Po-Wei Chen, Biodegradable green composites reinforced by the fiber recycling from disposable chopsticks, *Materials Science and Engineering: A* ,527- 6, (2010), Pages 1516-1521

- [54] Wang, H.M., Postle, R., Kessler, R.W., and Kessler, W., Removing pectin and lignin during chemical processing of hemp for textile applications. *Textile Research Journal*, 73(8): (2003) 664-669.
- [55] A. Gregorova , M. Hrabalova , R. Wimmer , B. Saake, C. Altaner, Poly(lactide acid) composites reinforced with fibers obtained from different tissue types of *Picea sitchensis*, *Journal of Applied Polymer Science*, 114 5 (2009)2616-2623
- [56] J .BIAGIOTTI, D.PUGLIA, L.TORRE, J.M. KENNY, A.ARBELAIZ, G. CANTERO, C.MARIETA, R.LLANO-PONTE, and I.MONDRAGON, A Systematic Investigation on the Influence of the Chemical Treatment of Natural Fibers on the Properties of Their Polymer Matrix Composites, *POLYMER COMPOSITES*(2004), Vol. 25, No. 5
- [57] [58] K.L.Pickering, G.W.Beckermann, S.N.Alam, N.J.Foreman Optimising industrial hemp fibre for composites, *Composites: Part A* 38 (2007) 461–468
- [59] Bessadok, A., Marais, S., Roudesli, S., Lixon, C., Metayer, M., Influence of chemical modifications on water-sorption and mechanical properties of Agave fibres, *Composites Part A(Applied Science and Manufacturing)*,39-1,(2008) 29-45
- [60] M. S. Huda, L. T. Drzal, A. K. Mohanty, and M. Misra, Effect of fiber surface- treatments on the properties of laminated biocomposites from poly(lactic acid) (PLA) and kenaf fibers, *Composites Science and Technology* 68 (2008) 424-432
- [61] M. Pluta, Morphology and properties of polylactide modified by thermal treatment, filling with layered silicates and plasticization, *Polymer* 45 (2004) 8239–8251
- [62] M. Chanda, S.K. Roy, *Plastics Technology Handbook*, Taylor and Francis (2006)
- [63] [64] Latif, L. and Saidpour, H., Assessment of plastic mixture quality in injection 16 – 3 moulding process. *Polymer Testing*, 1997. 241-258
- [65] G.Sui, M.A.Fuqua, C.A.Ulven, W.H.Zhong, A plant fiber reinforced polymer composite prepared by a twin-screw extruder, *Bioresource Technology* 100 (2009) 1246–1251
- [66] Kim, E.G., Park, J.K., and Jo, S.H., A study on fiber orientation during the injection molding of fiber-reinforced polymeric composites: (Comparison

- between image processing results and numerical simulation). *Journal of Materials Processing Technology*,. 111 1-3 (2001) 225-232
- [67] [68] Brooks, R., Injection molding based techniques, in *Comprehensive Composite Materials*, A. Kelly and C. Zweben, Editors. 2000, Elsevier Science Ltd: Oxford
- [69] Keller, A., Compounding and mechanical properties of biodegradable hemp fibre composites. *Composites Science and Technology*, 63-9 (2003) 1307-1316.
- [70] Karus, M. and Kaup, M., Natural fibres in the European automotive industry. *Journal of Industrial Hemp*, 7-1 (2002) 119-131
- [71] C. A. Harper, E. M. Petrie, *PLASTICS MATERIALS AND PROCESSES (A Concise Encyclopedia)*, Wiley-Interscience, 2003
- [72] Q. Zhou, M. Xanthos, Nanoclay and crystallinity effects on the hydrolytic degradation of polylactides, *Polymer Degradation and Stability* 93 (2008) 1450
- [73] [74] J.A. Brydson, *Plastic Materials (Seventh Edition)* Butterworth-Heinemann, (1999)
- [75] M. Todo, P. Sang Dae, K. Arakawa, and M. Koganemaru, Effect of crystallinity and loading-rate on mode I fracture behavior of poly(lactic acid), *Polymer* 47 (2006) 1357 - 1363
- [76] YEONG-TARNG SHIEH, HUI-CHUN CHUANG, DSC and DMA Studies on Silane-Grafted and Water-Crosslinked LDPE/LLDPE Blends, *Journal of Applied Polymer Science*, Vol. 81, (2001) 1808–1816
- [77] M.Y.Keating, L.B.Malone and W.D. Saunders, ANNEALING EFFECT ON SEMI-CRYSTALLINE MATERIALS IN CREEP BEHAVIOR, *Journal of Thermal Analysis and Calorimetry*,Vol.69 (2002)37–52
- [78] Milner, K.C., Anacker, R.L., Fukushi, K., Haskins, W.T., Landy, M., Malmgren, B., and Ribic, E., Structure and biological properties of surface antigens from gram-negative bacteria, in *Symposium on Relationship of Structure of Microorganisms to their Immunological Properties*. 1963: American Society for Microbiology, Cleveland, Ohio
- [79] Rowell, R.M., Han, J.S., and Rowell, J.S., Characterization and factors effecting fiber properties, in *Natural Polymers and Agrofibrils Composites*, E.L.A.L.a.M. Frolline, L.H.C., Editor. 2000, Embrapa Instrumentacao Agropecuaria: Sao Carlos, Brazil. p. 115-134.

- [80] Donald Garlotta, A Literature Review of Poly(Lactic Acid), *Journal of Polymers and the Environment*, Vol.9, No.2, (2002)
- [81] Klaus Friedrich, Stoyko Fakiro Zhong Zhang, *Polymer composites: from nano-to-macro-scale*, Springer, (2005)
- [82] P.Mutje, A.Lopez, M.E.Vallejos, J.P.Lopez, F.Vilaseca, Full exploitation of *Cannabis sativa* as reinforcement/filler of thermoplastic composite materials, *Composites: Part A* 38 (2007) 369–377
- [83] L. Y. Mwaikambo, and M. P. Ansell, Chemical modification of hemp, sisal, jute, and kapok fibers by alkalization, *Journal of Applied Polymer Science* 84 (2002) 2222.
- [84] A. P. Mathew, K. Oksman, and M. Sain, Mechanical properties of biodegradable composites from poly lactic acid (PLA) and microcrystalline cellulose (MCC), *Journal of Applied Polymer Science* 97 (2005) 2014-2025
- [85] Klaus Friedrich, Stoyko Fakiro Zhong Zhang, *Polymer composites: from nano-to-macro-scale*, Springer, (2005)
- [86] M.A.Sawpan K. L. Pickering, and A. Fernyhough, Hemp fibre reinforced Poly (lactic acid) composites, *Advanced Materials Research* 29-30 (2007) 337
- [87] Donald Garlotta, A Literature Review of Poly(Lactic Acid), *Journal of Polymers and the Environment*, Vol.9, No.2, (2002)
- [88] Standard Test Methods for Plane-Strain Fracture Toughness and Strain Energy Release Rate of Plastic Materials, ASTM D 5045 (1999).
- [89] Standard Test Method for Tensile Properties of Plastics, ASTM D 638-03(2003)
- [90] S. Pilla, S. Gong, E. O'Neill, R. M. Rowell, and A. M. Krzysik, Polylactide-pine wood flour composites, *Polymer Engineering and Science* 48 (2008) 578.
- [91] K.P. Menard, *Dynamic Mechanical Analysis 2nd Edition a Practical introduction*, CRC Press (2008)
- [92] M. Le Troedec, D. Sedan, C. Peyratout, J. P. Bonnet, A. Smith, R. Guinebretiere, V. Gloaguen, and P. Krausz, Influence of various chemical treatments on the composition and structure of hemp fibres, *Composites Part A: Applied Science and Manufacturing* 39 (2008) 514

- [93] M. Todo, P. Sang Dae, K. Arakawa, and M. Koganemaru, Effect of crystallinity and loading-rate on mode I fracture behavior of poly(lactic acid), *Polymer* 47 (2006) 1357 - 1363
- [94] N. Graupner, Improvement of the Mechanical Properties of Biodegradable Hemp Fiber Reinforced Poly(lactic acid)(PLA) Composites by the Admixture of Man-made Cellulose Fibers, *Journal of COMPOSITE MATERIALS*, Vol.43, No.06 (2009) 689- 702
- [95] P. Joung-Man, and K. Dae-Sik, The influence of crystallinity on interfacial properties of carbon and SiC two-fiber/polyetheretherketone (PEEK) composites, *Polymer Composites* 21 (2000) 789-797.
- [96] L. Y. Mwaikambo, and M. P. Ansell, Chemical modification of hemp, sisal, jute, and kapok fibers by alkalization, *Journal of Applied Polymer Science* 84 (2002) 2222.
- [97] P. Pengju, Z. Bo, K. Weihua, S. Serizawa, M. Iji, and Y. Inoue, Crystallization behavior and mechanical properties of bio-based green composites based on poly(L-lactide) and kenaf fiber, *Journal of Applied Polymer Science* 105 (2007) 1511-1518.
- [98] M. Pluta, and A. Galeski, Crystalline and supermolecular structure of polylactide in relation to the crystallization method, *Journal of Applied Polymer Science* 86 (2002) 1386-1397.
- [99] M. A. Sawpan, K. L. Pickering, and A. Fernyhough, Hemp fibre reinforced Poly (lactic acid) composites, *Advanced Materials Research* 29-30 (2007) 337
- [100] Hanwen Xiao, Wei Lu, Jen-Taut Yeh, Crystallization Behavior of Fully Biodegradable Poly(Lactic Acid)/Poly(Butylene Adipate-co-Terephthalate) Blends, *Journal of Applied Polymer Science*, 112 (2009) 3754–3763
- [101] S. J. Eichhorn, C. A. Baillie, N. Zafeiropoulos, L. Y. Mwaikambo, M. P. Ansell, A. Dufresne, K. M. Entwistle, P. J. Herrera-Franco, G. C. Escamilla, L. Groom, M. Hughes, C. Hill, T. G. Rials, and P. M. Wild, Current international research into cellulosic fibres, *Journal of Materials Science*, 36-9, (2001) 2107
- [102] P. Sang Dae, M. Todo, K. Arakawa, Effects of isothermal crystallization on fracture toughness and crack growth behavior of poly(lactic acid), *Journal of Materials Science* 40 (2005) 1055-1058

- [103] M. Todo, P. Sang Dae, K. Arakawa, and M. Koganemaru, Effect of crystallinity and loading-rate on mode I fracture behavior of poly(lactic acid), *Polymer* 47 (2006) 1357 - 1363
- [104] Y. H. Han, S. O. Han, D. Cho, and H.-I. Kim, Henequen/ unsaturated polyester biocomposites: Electron beam irradiation treatment and alkali treatment effects on the henequen fiber, *Macromolecular Symposia* 245-246 (2006) 539.
- [105] T. Williams, G. Allen, and M. S. Kaufman, The impact strength of fibre composites, *Journal of Materials Science* 8 (1973) 1765-1790
- [106] R.V. Silva, D. Spinelli, W.W.Bose Filho, S.Claro Neto, G.O. Chierice, J.R. Tarpani, Fracture toughness of natural fibers/castor oil polyurethane composites, *Composites Science and Technology* 66 (2006) 1328–1335
- [107] P. Joung-Man, and K. Dae-Sik, The influence of crystallinity on interfacial properties of carbon and SiC two-fiber/polyetheretherketone (PEEK) composites, *Polymer Composites* 21 (2000) 789.
- [108] A. P. Mathew, K. Oksman, and M. Sain, Mechanical properties of biodegradable composites from poly lactic acid (PLA) and microcrystalline cellulose (MCC), *Journal of Applied Polymer Science* 97 (2005) 2014-2025.
- [109] B. A. P. Ass, M. N. Belgacem, and E. Frollini, Mercerized linters cellulose: Characterization and acetylation in N,N-dimethylacetamide/lithium chloride, *carbohydrate Polymers* 63 (2006) 19-29
- [110] H. Cai, V. Dave, R. A. Gross, and S. P. McCarthy, Effects of physical aging, crystallinity, and orientation on the enzymatic degradation of poly(lactic acid), *Journal of Polymer Science, Part B: Polymer Physics* 34 (1996) 2701
- [111] S. Ouajai, and R. A. Shanks, Composition, structure and thermal degradation of hemp cellulose after chemical treatments, *Polymer Degradation and Stability* 89 (2005) 327.
- [112] D. Ray, and B. K. Sarkar, Characterization of alkali-treated jute fibers for physical and mechanical properties, *Journal of Applied Polymer Science* 80 (2001) 1013
- [113] Image of 3 point bending set up from Instron.
- [114] Image of DMA set up from perkin and elmer.
- [115] Cellulose structure - Brooker R.J., Widmaier E.P., Graham L.E. and Stiling P.D. 2008: Biology. McGraw-Hill. New York.

[116]

http://blogs.princeton.edu/chm333/f2006/biomass/bio_oil/02_chemistryprocessing_the_basics/01_chemistry/ lignin and hemicellulose

[117] <http://www1.lsbu.ac.uk/water/hypec.html> Pectin

[118] http://www.aist.go.jp/HNIRI/chap2/chap2_e.html PLA cycle

[119] http://www2.dupont.com/Plastics/en_US/Products/Zytel_HTN/Zytel_HTN_whitepaper_R8.html - polymer crystal structure

[120] Thomas Lundin; Steven M. Cramer; Robert H. Falk; and Colin Felton
Accelerated Weathering of Natural Fiber-Filled Polyethylene Composites
JOURNAL OF MATERIALS IN CIVIL ENGINEERING (2004) ASCE

Appendix 1- Data from fracture toughness testing, K_Q

Material / K_Q	Set 1	Set 2	Set 3	Set 4	Set 5	Mean
PLA Control	3.21	3.22	2.89	3.43	2.88	2.99
PLA 70°C 3Hrs	3.20	2.36	3.00	2.97	2.68	2.78
PLA 70°C 8Hrs	4.19	3.09	3.93	3.89	3.50	3.64
PLA 70°C 24Hrs	3.47	2.57	3.26	3.23	2.91	3.02
PLA 100°C 3Hrs	3.50	2.58	3.28	3.25	2.93	3.04
PLA 100°C 8Hrs	4.80	3.54	4.50	4.46	4.01	4.17
PLA 100°C 24Hr	4.14	3.06	3.89	3.85	3.47	3.60
15 wt% hemp/PLA control	3.04	2.24	2.85	2.82	2.54	2.64
15 wt% hemp/PLA 70°C 3Hrs	3.34	2.47	3.13	3.10	2.79	2.90
15 wt% hemp/PLA 70°C 8Hrs	2.08	1.54	1.95	1.94	1.74	1.81
15 wt% hemp/PLA 70°C 24Hrs	2.98	2.20	2.80	2.77	2.49	2.59
15 wt% hemp/PLA 100°C 3Hrs	2.68	1.98	2.52	2.49	2.24	2.33
15 wt% hemp/PLA 100°C 8Hrs	0.38	0.28	0.36	0.35	0.32	0.33
15 wt% hemp/PLA 100°C 24Hr	1.30	0.96	1.22	1.21	1.09	1.13
30 wt% hemp/ PLA Control	2.84	2.10	2.67	2.64	2.38	2.47
30 wt% hemp/PLA 70°C 3Hrs	3.45	2.55	3.24	3.21	2.89	3.00
30 wt% hemp/PLA 70°C 8Hrs	3.37	2.49	3.16	3.14	2.82	2.93
30 wt% hemp/PLA 70°C 24Hrs	2.76	2.04	2.59	2.57	2.31	2.40
30 wt% Hemp/PLA 100°C 3Hrs	2.82	2.08	2.65	2.62	2.36	2.45
30 wt% Hemp/PLA 100°C 8Hrs	2.56	1.90	2.41	2.39	2.15	2.23
30 wt% Hemp/PLA 100°C 24Hr	2.02	1.50	1.90	1.88	2.88	1.76

Appendix 1- Data from fracture toughness testing, K_{IC}

Material / K_Q	Set 1	Set 2	Set 3	Set 4	Set 5	Mean
PLA Control	2.05	1.51	1.60	1.90	1.83	1.78
PLA 70°C 3Hrs	1.96	1.45	1.53	1.82	1.75	1.7
PLA 70°C 8Hrs	2.54	1.88	1.99	2.36	2.28	2.21
PLA 70°C 24Hrs	2.00	1.48	1.57	1.86	1.79	1.74
PLA 100°C 3Hrs	2.10	1.56	1.65	1.96	1.88	1.83
PLA 100°C 8Hrs	3.00	2.22	2.35	2.79	2.69	2.61
PLA 100°C 24Hr	2.39	1.77	1.87	2.23	2.14	2.08
15 wt% hemp/PLA control	1.76	1.30	1.38	1.64	1.58	1.53
15 wt% hemp/PLA 70°C 3Hrs	2.01	1.49	1.58	1.87	1.80	1.75
15 wt% hemp/PLA 70°C 8Hrs	1.12	0.82	0.87	1.04	1.00	0.97
15 wt% hemp/PLA 70°C 24Hrs	1.81	1.33	1.41	1.68	1.62	1.57
15 wt% hemp/PLA 100°C 3Hrs	1.68	1.24	1.31	1.56	1.50	1.46
15 wt% hemp/PLA 100°C 8Hrs	0.41	0.31	0.32	0.39	0.37	0.36
15 wt% hemp/PLA 100°C 24Hr	0.78	0.58	0.61	0.73	0.70	0.68
30 wt% hemp/ PLA Control	1.70	1.26	1.33	1.58	1.52	1.48
30 wt% hemp/PLA 70°C 3Hrs	2.07	1.53	1.62	1.93	1.85	1.8
30 wt% hemp/PLA 70°C 8Hrs	2.06	1.52	1.61	1.92	1.84	1.79
30 wt% hemp/PLA 70°C 24Hrs	1.67	1.23	1.31	1.55	1.49	1.45
30 wt% Hemp/PLA 100°C 3Hrs	1.69	1.25	1.32	1.57	1.51	1.47
30 wt% Hemp/PLA 100°C 8Hrs	1.54	1.14	1.21	1.43	1.38	1.34
30 wt% Hemp/PLA 100°C 24Hr	1.14	0.84	0.89	1.06	1.02	0.99

Appendix 2 Data from tensile strength testing – Yield stress, σ_y

Material Type/ σ_y	Set 1	Set 2	Set 3	Set 4	Set 5	Mean /MPa
PLA Control	76.96	56.88	72.27	71.60	64.41	66.92
PLA 70°C 3Hrs	76.50	56.54	71.84	71.18	64.03	66.52
PLA 70°C 8Hrs	80.19	59.27	75.31	74.61	67.12	69.73
PLA 70°C 24Hrs	80.94	59.82	76.01	75.31	67.74	70.38
PLA 100°C 3Hrs	76.54	56.58	71.88	71.22	64.06	66.56
PLA 100°C 8Hrs	81.12	59.96	76.18	75.48	67.89	70.54
PLA 100°C 24Hr	78.84	58.28	74.04	73.36	65.99	68.56
15 wt% hemp/PLA control	73.20	54.10	68.74	68.11	61.26	63.65
15 wt% hemp/PLA 70°C 3Hrs	71.70	53.00	67.34	66.71	60.01	62.35
15 wt% hemp/PLA 70°C 8Hrs	70.55	52.15	66.26	65.64	59.05	61.35
15 wt% hemp/PLA 70°C 24Hrs	73.50	54.32	69.02	68.38	61.51	63.91
15 wt% hemp/PLA 100°C 3Hrs	72.50	53.58	68.08	67.45	60.68	63.04
15 wt% hemp/PLA 100°C 8Hrs	66.79	49.37	62.73	62.15	55.90	58.08
15 wt% hemp/PLA 100°C 24Hr	38.47	28.43	36.13	35.79	32.20	33.45
30 wt% hemp/ PLA Control	63.09	46.63	59.25	58.70	52.80	54.86
30 wt% hemp/PLA 70°C 3Hrs	64.19	47.45	60.29	59.73	53.73	55.82
30 wt% hemp/PLA 70°C 8Hrs	57.33	42.37	53.84	53.34	47.98	49.85
30 wt% hemp/PLA 70°C 24Hrs	81.02	59.88	76.09	75.38	67.81	70.45
30 wt% Hemp/PLA 100°C 3Hrs	55.84	41.28	52.44	51.96	46.74	48.56
30 wt% Hemp/PLA 100°C 8Hrs	48.36	35.74	45.41	44.99	40.47	42.05
30 wt% Hemp/PLA 100°C 24Hr	76.96	56.88	72.27	71.60	64.41	38.25

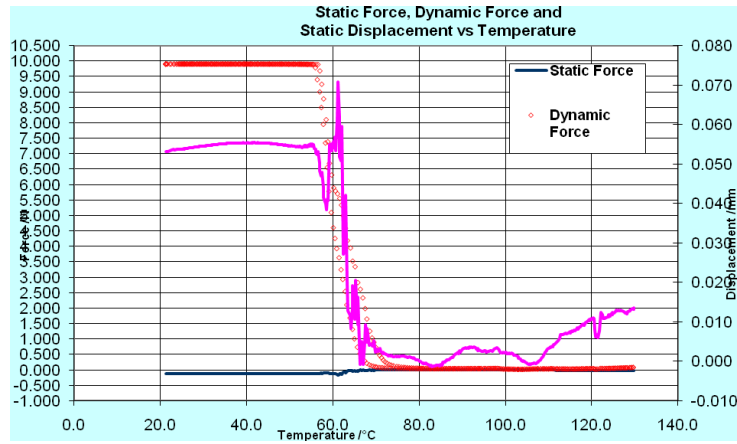
Appendix 3 Data from tensile strength testing – Young's Modulus, E

Material Type/ E	Set 1	Set 2	Set 31	Set 4	Set 5	Mean/Mpa
PLA Control	3472.37	2566.53	3261.01	3230.81	2906.22	3019.45
PLA 70°C 3Hrs	3612.73	2670.28	3392.82	3361.41	3023.69	3141.5
PLA 70°C 8Hrs	3857.42	2851.14	3622.62	3589.08	3228.49	3354.28
PLA 70°C 24Hrs	3744.77	2767.87	3516.83	3484.26	3134.21	3256.32
PLA 100°C 3Hrs	3724.71	2753.05	3497.99	3465.60	3117.42	3238.88
PLA 100°C 8Hrs	4190.67	3097.45	3935.58	3899.14	3507.41	3644.06
PLA 100°C 24Hr	4833.69	3572.73	4539.47	4497.43	4045.59	4203.21
15 wt% hemp/PLA control	4675.16	3455.56	4390.59	4349.94	3912.91	4065.36
15 wt% hemp/PLA 70°C 3Hrs	4836.00	3574.44	4541.64	4499.59	4047.52	4205.22
15 wt% hemp/PLA 70°C 8Hrs	4536.14	3352.80	4260.03	4220.58	3796.55	3944.47
15 wt% hemp/PLA 70°C 24Hrs	5003.62	3698.32	4699.05	4655.54	4187.81	4350.97
15 wt% hemp/PLA 100°C 3Hrs	4863.84	3595.02	4567.78	4525.49	4070.83	4229.43
15 wt% hemp/PLA 100°C 8Hrs	5506.66	4070.14	5171.47	5123.59	4608.84	4788.4
15 wt% hemp/PLA 100°C 24Hr	5868.06	4337.26	5510.87	5459.85	4911.31	5102.66
30 wt% hemp/ PLA Control	7043.32	5205.94	6614.60	6553.35	5894.96	6124.63
30 wt% hemp/PLA 70°C 3Hrs	7149.69	5284.55	6714.49	6652.32	5983.98	6217.12
30 wt% hemp/PLA 70°C 8Hrs	6718.36	4965.74	6309.41	6250.99	5622.97	5842.05
30 wt% hemp/PLA 70°C 24Hrs	5801.67	4288.19	5448.52	5398.08	4855.75	5044.93
30 wt% Hemp/PLA 100°C 3Hrs	7114.16	5258.30	6681.13	6619.27	5954.25	6186.23
30 wt% Hemp/PLA 100°C 8Hrs	7128.07	5268.57	6694.19	6632.20	5965.88	6198.32
30 wt% Hemp/PLA 100°C 24Hr	3472.37	2566.53	3261.01	3230.81	2906.22	6300.7

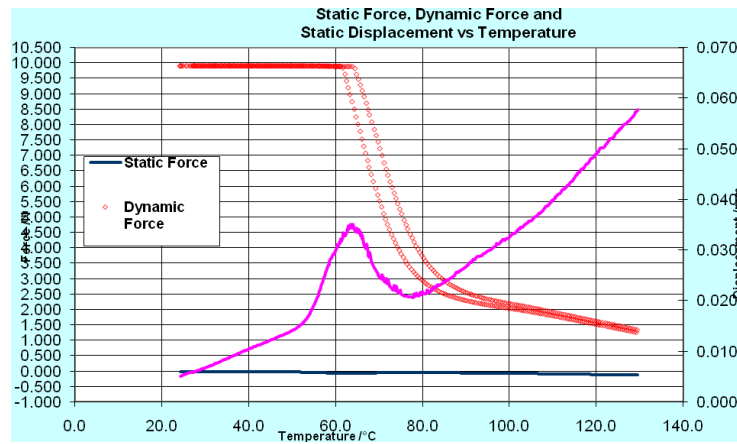
Appendix 4 Data from tensile strength testing – Yield Strain, ϵ

Material Type/ ϵ	Set 1	Set 2	Set 31	Set 4	Set 5	Mean
PLA Control	3.73	2.75	3.50	3.47	3.12	3.24
PLA 70°C 3Hrs	4.58	3.38	4.30	4.26	3.83	3.98
PLA 70°C 8Hrs	3.37	2.49	3.16	3.14	2.82	2.93
PLA 70°C 24Hrs	2.14	1.58	2.01	1.99	1.79	1.86
PLA 100°C 3Hrs	2.96	2.18	2.78	2.75	2.47	2.57
PLA 100°C 8Hrs	2.78	2.06	2.61	2.59	2.33	2.42
PLA 100°C 24Hr	1.53	1.13	1.44	1.42	1.28	1.33
15 wt% hemp/PLA control	2.28	1.68	2.14	2.12	1.91	1.98
15 wt% hemp/PLA 70°C 3Hrs	2.32	1.72	2.18	2.16	1.94	2.02
15 wt% hemp/PLA 70°C 8Hrs	2.81	2.07	2.64	2.61	2.35	2.44
15 wt% hemp/PLA 70°C 24Hrs	2.15	1.59	2.02	2.00	1.80	1.87
15 wt% hemp/PLA 100°C 3Hrs	1.90	1.40	1.78	1.77	1.59	1.65
15 wt% hemp/PLA 100°C 8Hrs	1.54	1.14	1.45	1.43	1.29	1.34
15 wt% hemp/PLA 100°C 24Hr	0.78	0.58	0.73	0.73	0.65	0.68
30 wt% hemp/ PLA Control	1.00	0.74	0.94	0.93	0.84	0.87
30 wt% hemp/PLA 70°C 3Hrs	1.02	0.76	0.96	0.95	0.86	0.89
30 wt% hemp/PLA 70°C 8Hrs	1.16	0.86	1.09	1.08	0.97	1.01
30 wt% hemp/PLA 70°C 24Hrs	2.10	1.56	1.98	1.96	1.76	1.83
30 wt% Hemp/PLA 100°C 3Hrs	0.86	0.64	0.81	0.80	0.72	0.75
30 wt% Hemp/PLA 100°C 8Hrs	0.93	0.69	0.87	0.87	0.78	0.81
30 wt% Hemp/PLA 100°C 24Hr	3.73	2.75	3.50	3.47	3.12	0.51

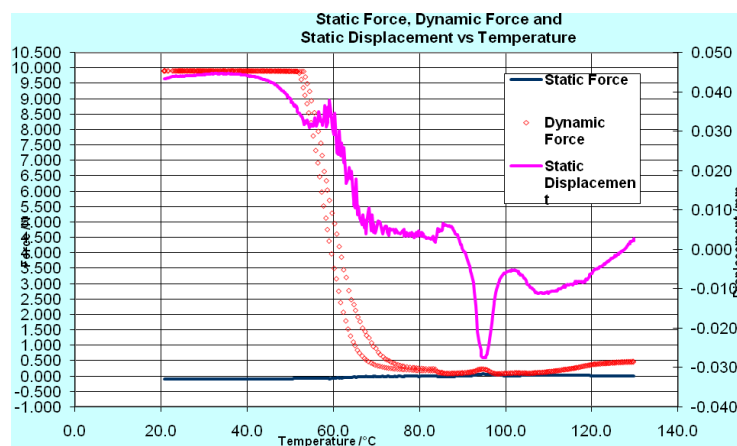
Appendix 5
 Data from Dynamic Mechanical Thermal Analysis testing
 Static and Dynamic Force, with Static Displacement graphs



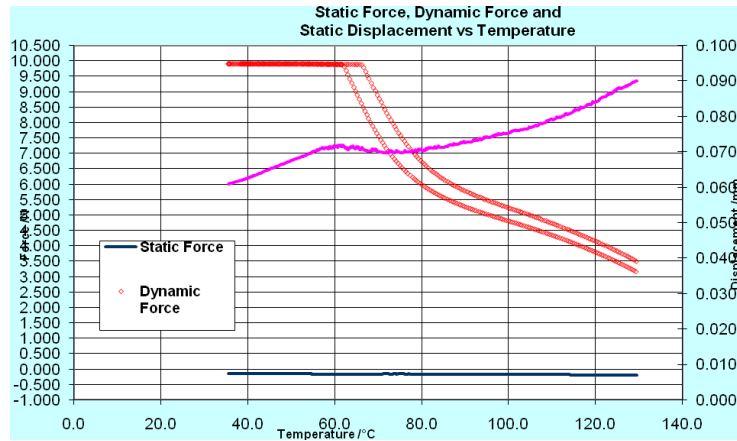
PLA control



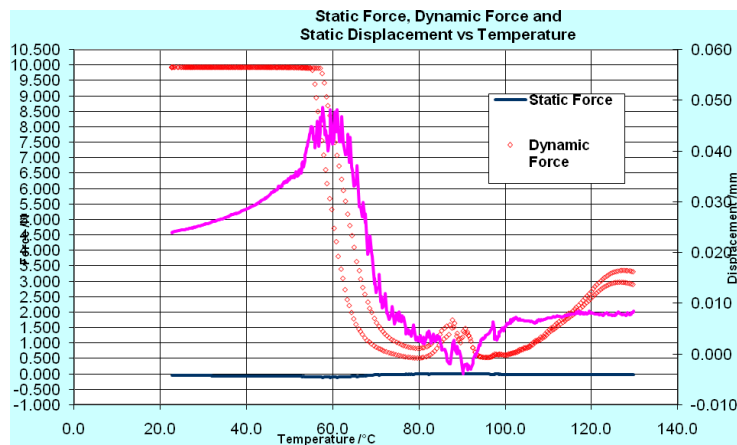
. PLA 100°C 24 Hours



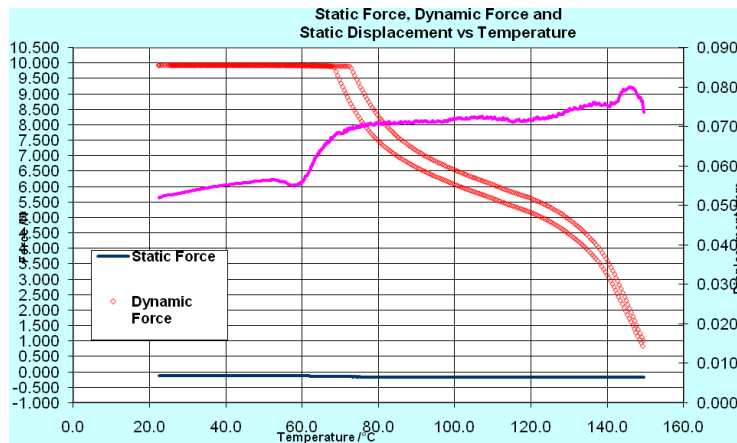
15 wt% hemp/PLA control



15 wt% hemp/PLA 100°C 24 hours



30 wt% hemp/PLA control



30 wt% hemp/PLA 100°C 24 hours

Appendix 6 – Data from X-ray diffraction testing

Type of Composite	Intensity, I_{002}	Intensity, I_{amp}
PLA control	-	-
PLA 100°C 24hrs	-	-
15 wt % hemp/PLA control	491	328
15 wt % hemp/PLA 100°C 24 hours	619	259
30 wt % hemp/PLA control	669	315
30 wt % hemp/PLA 100°C 24 hours	247	135